Journal of Sound and Vibration 329 (2010) 4068–4092

Contents lists available at ScienceDirect

Journal of Sound and Vibration

journal homepage: www.elsevier.com/locate/jsvi

Crowd-induced random vibration of footbridge and vibration control using multiple tuned mass dampers

Quan Li, Jiansheng Fan *, Jianguo Nie, Quanwang Li, Yu Chen

Department of Civil Engineering, Tsinghua University, Beijing 100084, China

ARTICLE INFO

Article history:
Received 17 April 2009
Received in revised form
10 April 2010
Accepted 13 April 2010
Handling Editor: S. Ilanko

ABSTRACT

This paper investigates vibration characteristics of footbridge induced by crowd random walking, and presents the application of multiple tuned mass dampers (MTMD) in suppressing crowd-induced vibration. A single foot force model for the vertical component of walking-induced force is developed, avoiding the phase angle inaccessibility of the continuous walking force. Based on the single foot force model, the crowd–footbridge random vibration model, in which pedestrians are modeled as a crowd flow characterized with the average time headway, is developed to consider the worst vibration state of footbridge. In this random vibration model, an analytic formulation is developed to calculate the acceleration power spectral density in arbitrary position of footbridge with arbitrary span layout. Resonant effect is observed as the footbridge natural frequencies fall within the frequency bandwidth of crowd excitation. To suppress the excessive acceleration for human normal walking comfort, a MTMD system is used to improve the footbridge dynamic characteristics. According to the random vibration model, an optimization procedure, based on the minimization of maximum root-mean-square (rms) acceleration of footbridge, is introduced to determine the optimal design parameters of MTMD system. Numerical analysis shows that the proposed MTMD designed by random optimization procedure, is more effective than traditional MTMD design methodology in reducing dynamic response during crowd–footbridge resonance, and that the proper frequency spacing enlargement will effectively reduce the off-tuning effect of MTMD.

1. Introduction

With the rapid development of high-performance materials and the flourish of bridge construction in China, there has been a trend towards long-span footbridge characterized with light weight, slenderness and low natural frequency. When external loads due to crowd walking act on the footbridge, it may suffer from excessive vibration that inhibits the normal walking and causes pedestrian discomfort.

The excessive footbridge vibration due to the pedestrian passage is a major consideration in the footbridge design. To understand the complicated mechanical mechanism of pedestrian-footbridge resonance and develop rational and reasonable design procedures, a number of numerical and experimental investigations have been performed over the past decades. In those studies, one of the main subjects was mathematical modeling of human-induced dynamic forces. Generally, the dynamic force induced by a pedestrian is represented by Fourier series with constant period [1]. Many scholars

* Corresponding author.
E-mail address: fanjsh@tsinghua.edu.cn (J.S. Fan).

0022-460X/$ - see front matter © 2010 Elsevier Ltd. All rights reserved.
doi:10.1016/j.jsv.2010.04.013

Nomenclature

a_{rms} rms acceleration of footbridge
A_n Fourier coefficient in the single foot force formulation
c_i dynamic load factor of the ith harmonic
c_{tl} the damping coefficient of the lth TMD
f_s stride rate of pedestrian
f_{si} the stride rate of the ith pedestrian
$F(x,t)$ the crowd loading function
$F_c(t)$ the continuous walking force
$F_e(t)$ the single foot force
$F_{ei}(t)$ the single foot force of the ith pedestrian
$F_n(t)$ the nth modal load function of footbridge generated by crowd crossing
$F_{n,\mathrm{MTMD}}(t)$ the nth modal load function of footbridge generated by MTMD
$F_s(t)$ the loading time history in the foot standing point
G body weight of pedestrian
k_{tl} the stiffness of the lth TMD
K the total number of foot standing points on the footbridge
L the span of footbridge
m_{tl} the mass of the lth TMD
M_n the nth modal mass of footbridge
N total number of pedestrians from the left end
N' total number of pedestrians from the right end
p the total number of TMD
$q_n(t)$ the nth modal displacement of footbridge
$S_{F_n}(\omega)$ the power spectral density of the nth modal force
$S_{F_s}(\omega)$ the power spectral density of the loading time history in the first foot standing point
$S_{q_n}(\omega)$ the power spectral density of the nth flexural modal displacement
$S_{\ddot{q}_n}(\omega)$ the power spectral density of the nth flexural modal acceleration
$S_{\ddot{u}}(x,\omega)$ the acceleration power spectral density of footbridge at section x
t_i the time when the ith pedestrian walks onto the footbridge
T the average time interval of crowd flow
T_e constant cycle of single foot force
T_s the cycle of the continuous walking force
$u(x,t)$ the vertical displacement of footbridge
$U(t)$ the unit step function
v_{tl} the stroke of the lth TMD
x_t the installation position of MTMD on the footbridge
$z_{tl}(t)$ the vertical displacement of the lth TMD

β_{tl} the modal frequency ratio of the lth TMD
$\delta(x)$ the Dirac delta function
Δl the stride length of pedestrian
ΔT the lag time of the crowd flow from the right after that from the left
ξ_n the nth modal damping ratio of footbridge
ξ_{tl} the damping ratio of the lth TMD
υ walking speed of crowd flow
υ_i walking speed of the ith pedestrian
$\phi_n(x)$ the nth modal coordinate at section x
φ_i phase angle of the ith harmonic
ω_n the nth modal circular frequency of footbridge
ω_{tl} the circular frequency of the lth TMD

put forward various formulations of dynamic load factor (DLF) and phase angle of each harmonic, from which the walking force are determined [1–6]. Subsequently, the probabilistic force model [7,8] and frequency-domain force model [9,10] are developed as two typical models to evaluate the random characteristics of the walking force.

Though most of previous researches recognized the dynamic behaviors of footbridge, the crowd excitation corresponding to the serviceability state, was not well addressed. Investigations of footbridge vibration under crowd-induced moving loads are relatively few [8,10–14], especially the random vibration of footbridge considering the pedestrians' random passing sequence and variability of stride rates. Matsumoto [11] examines the characteristics of dynamic fluctuation of pedestrian's load, and developed the statistical relationship between the collective effect of crowd and the individual effect of pedestrian on the vibration response of footbridge. Fujino et al. [14] observed the human-induced large-amplitude lateral vibration of an actual bridge in the congested condition, and studied the influence of pedestrians' lateral resonant forces resulting from walking synchronization to the lateral vibration. Brownjohn et al. [10] presented an auto-spectral density function to describe the realistically imperfect walking force, and adopted the stochastic vibration approach to calculate the footbridge vibration under crowd loading in the frequency domain. Venuti et al. [13] modeled the dynamics of the crowd as a compressive flow, and proposed a mathematical model to calculate the vibration of footbridge under crowd-induced excitation. These researches qualitatively depicted the effect of crowd excitations on the vibration of footbridge and explored the possibility of solving the crowd–footbridge vibration from the random vibration approach; however, a general crowd–footbridge random vibration model has not been put forward.

When pedestrians cross footbridge with uniform stride rate and in a congested state, the excessive vibration is likely to appear and exceeds the walking comfort requirement of pedestrians. Thus, it is essential to find an appropriate and applicable approach to reduce such vibration. As a relatively economical and convenient vibration control system, the passive multiple tuned mass dampers (MTMD) can effectively reduce the response contribution of the controlled structure mode without much interference to the dynamic characteristics of original structure when properly tuned. Xu and Igusa [15] commended the application of MTMD system to suppressing the excessive vibration of single-degree-of-freedom

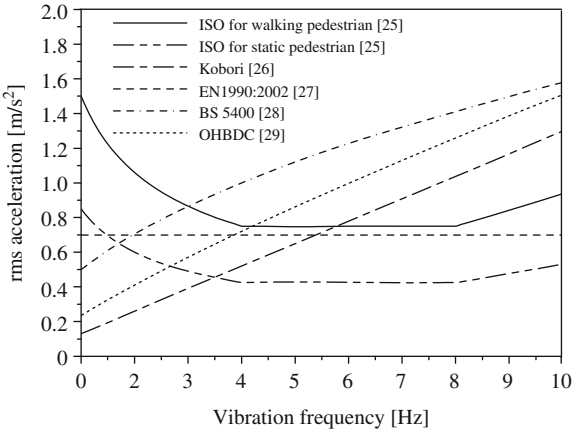

Fig. 1. Illustrations of footbridge vibration comfort requirement employed by various codes.

system under wide-band random excitation. Yamaguchi and Harnpornchai [16] discussed the fundamental characteristics of MTMD to suppress harmonically forced oscillations, including the frequency range, TMD damping ratio, and total number of TMDs, and further advised some design considerations of MTMD system. Subsequent studies on the vibration suppression effectiveness of MTMD are performed in wind-induced vibration of bridge structures [17], and coupled train-bridge or vehicle-bridge vibration [18,19], and it is observed that the MTMD system suppresses excessive vibration more effectively and provides better robustness than a single TMD. Several researchers have investigated its practical applications in suppressing footbridge vibration due to pedestrian passing and emphasized on the robustness of its control performance due to the off-tuning effect. Bachmann and Weber [20] proposed the optimal procedure to determine the design parameters of TMD for lightly damped structures, and demonstrated that the effectiveness of TMD was much more sensitive to the error in the tuning of the TMD frequency than that in the tuning of its damping. Poovarodom et al. [21–23] presented the application of MTMD system to suppress man-induced vibrations of a footbridge, and examined the sensitivity of the control effectiveness of MTMD system against estimation errors in the footbridge's natural frequency and magnitude of pedestrian load. However, only the footbridge vibration generated by a single pedestrian passing was shown to illustrate MTMD control effectiveness. It is interesting to explore its performance under crowd passing with uniform and random stride rates, and this is one of the main objectives of this study.

In this study, the single foot force formulation which can account for the different stride rates is firstly proposed. With this formulation, the complex crowd–footbridge resonant vibration mechanism is revealed from the random vibration approach and a highly efficient computing model in the frequency domain is developed to calculate such vibration. For the walking comfort of pedestrians, the rms acceleration of footbridge should accord with the vibration comfort requirements in the serviceability state [24–29] and these requirements are illustrated in Fig. 1. Most of comfort requirement curves are frequency-dependent. Thus, according to the objective of minimizing the footbridge rms acceleration, an optimal design procedure of MTMD system is developed to suppress excessive footbridge vibration under passing crowd with uniform or random stride rates. The footbridge natural frequency fluctuation induced by crowd–footbridge interactions under congested crowd passing is studied, and the MTMD off-tuning effect resulting from the estimation error or time variation of footbridge natural frequencies is investigated. Illustrated examples have been provided to verify the validity of the developed methodology.

2. A loading model for walking pedestrian

2.1. Single foot force model

Accurate evaluation of vertical force induced by one walking pedestrian is crucial to estimate the vibration of footbridge. The continuous walking force, associated with the vertical oscillation of the body center of mass, is often modeled as a sum of a static and a dynamic component as [30]

$$F_c(t) = G + \sum_{i=1}^{n} Ga_i \cos(2\pi i f_s t) + \sum_{i=1}^{n} Gb_i \sin(2\pi i f_s t) = G + \sum_{i=1}^{n} Gc_i \sin(2\pi i f_s t + \varphi_i), \quad i = 1,2,\ldots,n \tag{1}$$

where f_s is the stride rate, G is the body weight, and c_i and φ_i are the dynamic load factor (DLF) and the phase angle of the ith harmonic, respectively.

With the advancement of experimental technology, many scholars have carried on a series of measurements to identify the various parameters (f_s, c_i and φ_i) to evaluate $F_c(t)$ based on Eq. (1). Many scholars carried out a series of walking force

measurements to obtain the DLFs within the normal stride rate range [4,6,30,31]. Among them, Young's empirical equation [6], based on a regression of available tested vertical forces (including Kerr' results [5]), evaluates the first four orders of DLFs with 75 percent assurance rate, as showed in Eq. (2). In terms of stride rate, Matsumoto [32], based on 505 samples of the vertical force curves, summarized that stride rates basically accorded with the normal distribution with mean 2.0 Hz, and standard deviation 0.173 Hz, and that 1.6–2.4 Hz basically covered the common range of stride rates. However, since the phase angle does not have a clear physical meaning, its definite statistical law has not well been detected:

$$c_1 = 0.41(f_s - 0.95) \le 0.56, \quad f_s = 1-2.8\,\text{Hz}$$

$$c_2 = 0.069 + 0.0056 \times 2f_s, \quad 2f_s = 2-5.6\,\text{Hz}$$

$$c_3 = 0.033 + 0.0064 \times 3f_s, \quad 3f_s = 3-8.4\,\text{Hz}$$

$$c_4 = 0.013 + 0.0065 \times 4f_s, \quad 4f_s = 4-11.2\,\text{Hz} \tag{2}$$

Without the applicable rule of phase angle, it is difficult for Eq. (1) to take into practice. Therefore, this paper develops a single foot force model to describe the dynamic loading of pedestrian walking, not only avoiding the inaccessibility of phase angle and also accounting for subsequent random vibration modeling of footbridge. Generally, the common single foot load–time force curve, illustrated in Fig. 2, is characterized with two peaks, and the first one is higher than the second one.

Since foot standing points constantly change their positions on the footbridge when pedestrian walks, the single foot force is more realistic to evaluate footbridge dynamic response than the continuous walking force. In view of the universality and preciseness of load model, Young's empirical equation of DLFs is chosen to construct the single foot force model.

The single foot force is assumed to be formulated by Fourier series as

$$F_e(t) = G\sum_{n=1}^{+\infty} A_n \sin\left(\frac{\pi n}{T_e}t\right), \quad 0 \le t \le T_e \tag{3}$$

where A_n and T_e is the Fourier coefficient and constant cycle. Due to the limited number of constraint equations relating the single force model with the continuous walking force, only the first five order Fourier coefficients are considered in the single foot force model, for the DLFs of only the first four harmonics are available according to previous studies and walking force measures. According to the statistical result of Ebrahimpour [7], the ratio of the cycle of single foot force to the period during which both feet have contact with ground is basically unchanged, and this ratio is approximately 4.165 on average. Thus, illustrated by Fig. 3, the cycle of the continuous walking force which is the inverse of stride rate is written as

$$\frac{T_e}{\Delta t} = 4.165 \rightarrow \Delta t = 0.24T_e$$

$$T_s = T_e - \Delta t = 0.76T_e \tag{4}$$

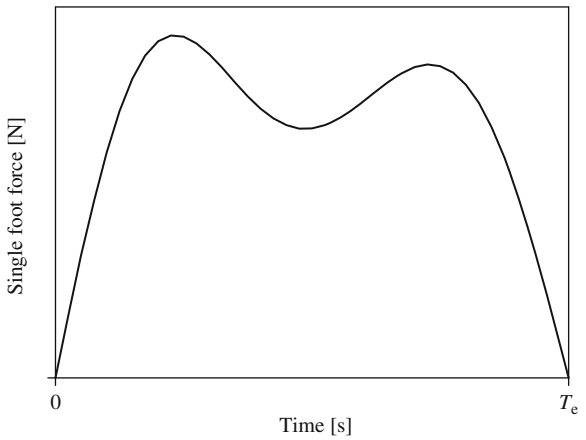

Fig. 2. Single foot load–time force curve.

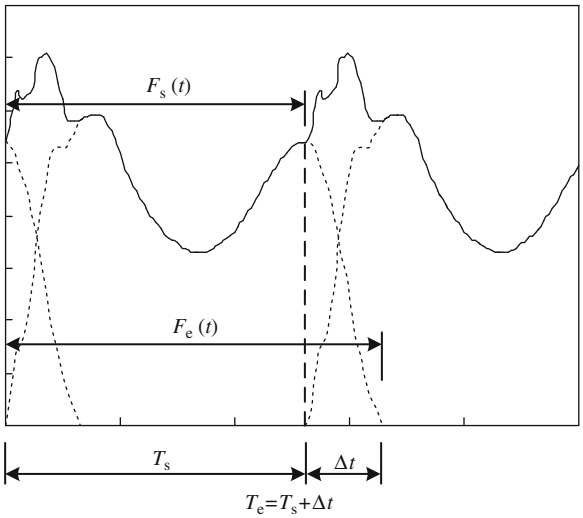

Fig. 3. Construction of the continuous walking force by superposing the single foot force in the time domain.

The continuous walking force in its constant cycle could be determined by the single foot force as

$$\begin{cases} F_c(t) = G\sum_{n=1}^{5} A_n\left\{\sin\left(\frac{\pi n}{T_e}t\right)+\sin\left[\frac{\pi n}{T_e}(t+T_s)\right]\right\}, & t\in[0,0.24T_e] \\ F_c(t) = G\sum_{n=1}^{5} A_n \sin\left(\frac{\pi n}{T_e}t\right), & t\in[0.24T_e,0.76T_e] \end{cases} \tag{5}$$

In addition, the continuous walking force with the cycle of $0.76T_e$ could be expressed as

$$F_c(t) = G+\sum_{i=1}^{n} Ga_i\cos\left(\frac{2\pi i}{0.76T_e}t\right)+\sum_{i=1}^{n} Gb_i\sin\left(\frac{2\pi i}{0.76T_e}t\right) = G+\sum_{i=1}^{n} Gc_i\sin\left(\frac{2\pi i}{0.76T_e}t+\varphi_i\right), \quad i=1,2,\ldots,n \tag{6}$$

Combining Eqs. (5) and (6), the Fourier coefficients in the single foot model could be calculated by

$$\begin{cases} \sum_{n=1}^{5}\left[\int_0^{0.76T_e}\sin\left(\frac{\pi n}{T_e}t\right)dt\right]A_n+\sum_{n=1}^{5}\left[\int_0^{0.24T_e}\sin\left[\frac{\pi n}{T_e}(t+0.76T_e)\right]dt\right]A_n = 0.76T_e \\ \sum_{n=1}^{5}\left[\int_0^{0.76T_e}\cos\left(\frac{2\pi i}{0.76T_e}t\right)\sin\left(\frac{\pi n}{T_e}t\right)dt\right]A_n+\sum_{n=1}^{5}\left[\int_0^{0.24T_e}\cos\left(\frac{2\pi i}{0.76T_e}t\right)\sin\left[\frac{\pi n}{T_e}(t+0.76T_e)\right]dt\right]A_n = 0.38T_e a_i \\ \sum_{n=1}^{5}\left[\int_0^{0.76T_e}\sin\left(\frac{2\pi i}{0.76T_e}t\right)\sin\left(\frac{\pi n}{T_e}t\right)dt\right]A_n+\sum_{n=1}^{5}\left[\int_0^{0.24T_e}\sin\left(\frac{2\pi i}{0.76T_e}t\right)\sin\left[\frac{\pi n}{T_e}(t+0.76T_e)\right]dt\right]A_n = 0.38T_e b_i \\ \sqrt{a_i^2+b_i^2}=c_i, \quad i=1,2,3,4 \end{cases} \tag{7}$$

According to three constraint conditions: (1) $F_e(t)$ is always the significant positive value in its cycle; (2) A_n is the real number; (3) the single foot force calculated by Eq. (3) is similar to the experimental force curve with two peaks and the first one higher than the second one, the solution of this equation set is demonstrated as Fig. 4. And then by the least-square method, the convenient expression of Fourier coefficients is written as

$$A_1 = \begin{cases} -0.0698f_s+1.211, & 1.6\,\text{Hz}\le f_s\le 2.32\,\text{Hz} \\ -0.1784f_s+1.463, & 2.32\,\text{Hz}< f_s\le 2.4\,\text{Hz} \end{cases}$$

$$A_2 = \begin{cases} 0.1052f_s-0.1284, & 1.6\,\text{Hz}\le f_s\le 2.32\,\text{Hz} \\ -0.4716f_s+1.210, & 2.32\,\text{Hz}< f_s\le 2.4\,\text{Hz} \end{cases}$$

$$A_3 = \begin{cases} 0.3002f_s-0.1534, & 1.6\,\text{Hz}\le f_s\le 2.32\,\text{Hz} \\ -0.0118f_s+0.5703, & 2.32\,\text{Hz}< f_s\le 2.4\,\text{Hz} \end{cases}$$

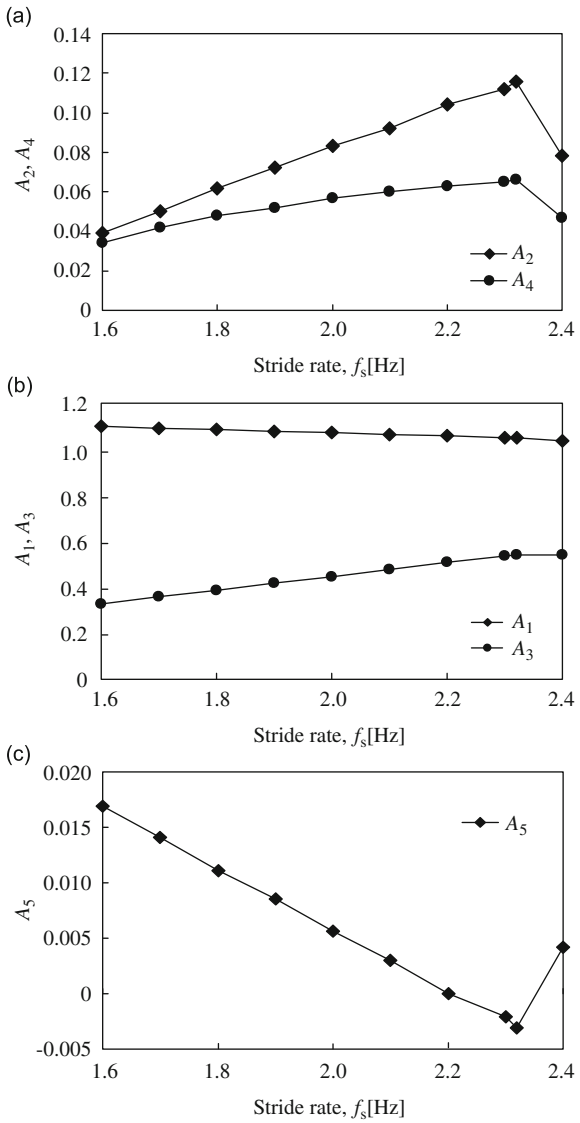

Fig. 4. A_1, A_2, A_3, A_4 and A_5 in the common stride rate range (1.6–2.4 Hz). (a) A_2 and A_4. (b) A_1 and A_3. (c) A_5.

$$A_4 = \begin{cases} 0.0416f_s - 0.0288, & 1.6\,\text{Hz} \le f_s \le 2.32\,\text{Hz} \\ -0.2600f_s + 0.6711, & 2.32\,\text{Hz} < f_s \le 2.4\,\text{Hz} \end{cases}$$

$$A_5 = \begin{cases} -0.0275f_s + 0.0608, & 1.6\,\text{Hz} \le f_s \le 2.32\,\text{Hz} \\ 0.0906f_s - 0.2132, & 2.32\,\text{Hz} < f_s \le 2.4\,\text{Hz} \end{cases} \quad (8)$$

2.2. Verification of the single foot force model

The single foot forces, together with the continuous walking forces constructed by the single foot force model are compared with various measured forces [5,7,12,30], as shown in Fig. 5. From the comparison, it is apparently shown that the various force histories constructed by the single foot force model accord with the measured ones for the most part. Additionally, the slight discrepancy between them lies in: (1) the DLFs of four harmonics recommended by Young are resulted from statistical regression; (2) the cycle of the continuous walking force deduced from Ebrahimpour's study is also statistically significant; (3) the discreteness of measured forces due to different measuring techniques plays a non-ignorable influence.

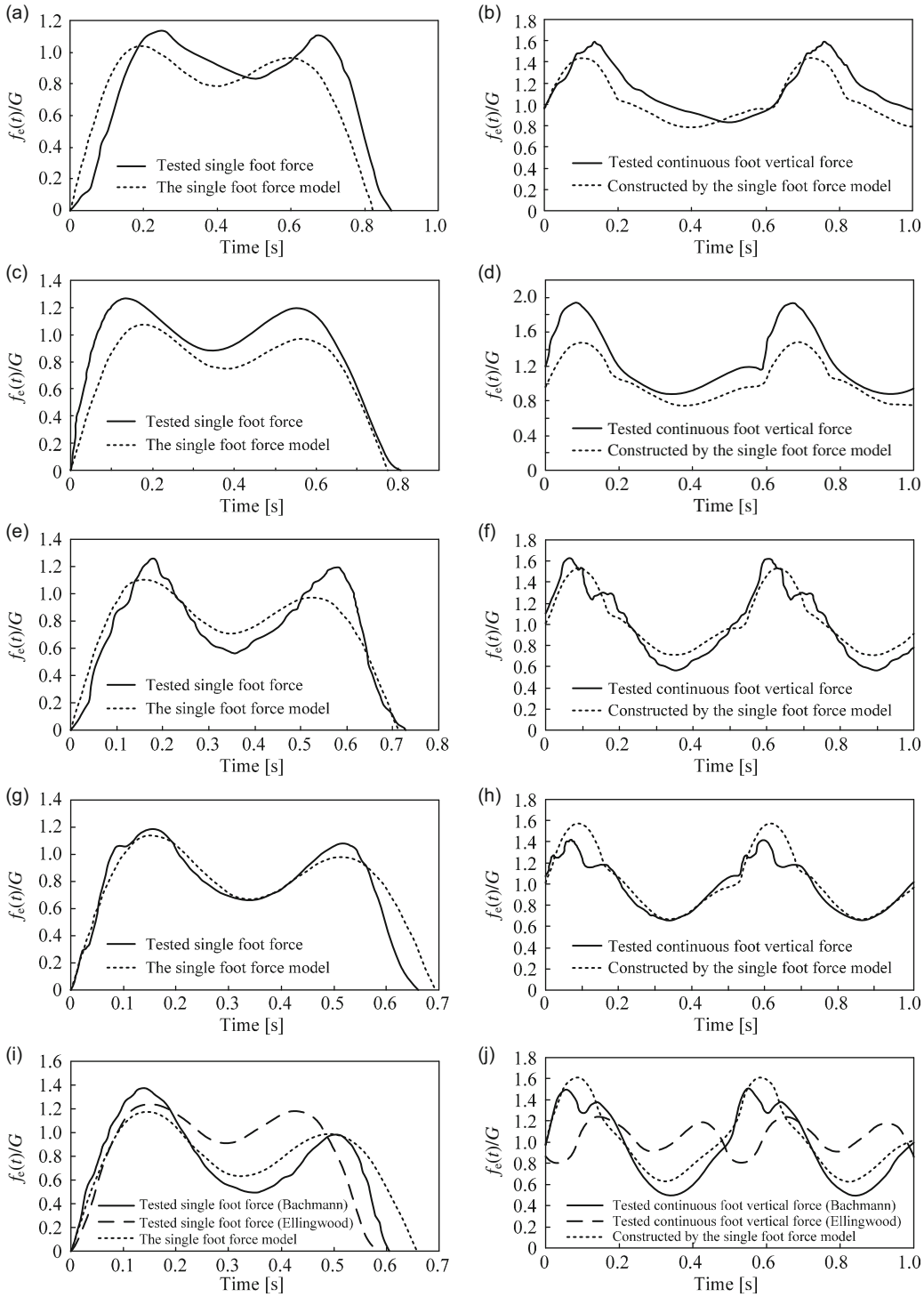

Fig. 5. Comparison of the single foot model and measured walking forces. (a) Comparison of the single foot model and Kerr's measured single foot force (f_s=1.6 Hz). (b) Comparison of the single foot model and Kerr's measured continuous walking force (f_s=1.6 Hz). (c) Comparison of the single foot model and Ellingwood's measured single foot force (f_s=1.7 Hz). (d) Comparison of the single foot model and Ellingwood's measured continuous walking force (f_s=1.7 Hz). (e) Comparison of the single foot model and Ebrahimpour's measured single foot force (f_s=1.85 Hz). (f) Comparison of the single foot model and Ebrahimpour's measured continuous walking force (f_s=1.85 Hz). (g) Comparison of the single foot model and Kerr's measured single foot force (f_s=1.9 Hz). (h) Comparison of the single foot model and Kerr's measured continuous walking force (f_s=1.9 Hz). (i) Comparison of the single foot model and Bachmann's and Ellingwood's measured single foot force (f_s=2.0 Hz). (j) Comparison of the single foot model and Bachmann's and Ellingwood's measured continuous walking force (f_s=2.0 Hz).

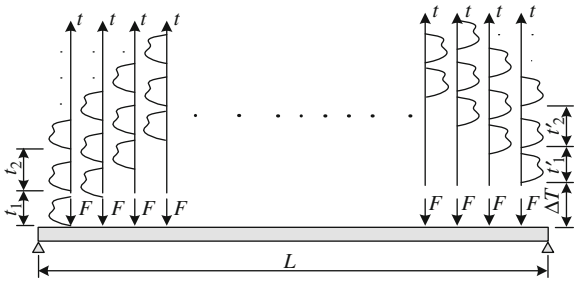

Fig. 6. Crowd-induced excitation on the footbridge.

3. Crowd-induced vibration of footbridge in the time domain

The flexural motion of footbridge at section x is [33]

$$\frac{\partial^2}{\partial x^2}\left(EI\frac{\partial^2 u(x,t)}{\partial x^2}\right)+m\frac{\partial^2 u(x,t)}{\partial t^2}+c\frac{\partial u(x,t)}{\partial t}=F(x,t) \tag{9}$$

where EI, m, c, and $u(x,t)$ are the stiffness, linear density, viscous damping coefficient and vertical displacement of footbridge, respectively; $F(x,t)$ is the external loading. Assuming the stride length is constant, Fig. 6 demonstrates the crowd-induced excitation of a footbridge spatially and temporally. Corresponding to the fact that the ith pedestrian begins to walk onto the footbridge from $x=x_i$ $(0\le x_i\le \Delta l)$ at the time $t=t_i$ from the left, and that from the right the ith pedestrian begins to walk onto footbridge from $x=x_{i'}$ $(0\le x_i\le \Delta l)$ at the time $t=t_{i'}$, the crowd loading function is written as

$$F(x,t)=\sum_{i=1}^{N}\sum_{k=1}^{K}\delta[x-(k-1)\Delta l-x_i]F_{ei}[t-(k-1)t_{si}-t_i]H(t,t_i)+\sum_{i'=1}^{N'}\sum_{j=1}^{K}\delta[x-(L-(k-1)\Delta l-x_{i'})]F_{ei'}[t-(k-1)t_{si'}-t_{i'}-\Delta T]H(t,t_{i'}) \tag{10}$$

where $H(t,t_i)=U(t-t_i)-U(t-(t_i+L/v_i))$; $F_{ei}(t)$ and $F_{ei'}(t)$ are the single foot forces of the ith pedestrian from the left and the ith one from the right; and $U(t)$ and $\delta(x)$, respectively, represent the unit step function and the Dirac delta function, which are individually defined as

$$\int_{-\infty}^{\infty}\delta(x)\,\mathrm{d}x=\begin{cases}1, & x=0\\ 0, & x\neq 0\end{cases} \tag{11}$$

$$U(t)=\begin{cases}1, & t\ge 0\\ 0, & t<0\end{cases} \tag{12}$$

In Eq. (10), Δl, L and K, represent the stride length, the span of footbridge and the total number of foot standing points on the footbridge, respectively. N and N' are the total number of pedestrians from the left and the right. t_{si} and $t_{si'}$ are the ith pedestrian's cycle of the single foot force from the left and the ith pedestrian's cycle from the right. ΔT is the lag time of the crowd flow from the right after that from the left. According to Eq. (9), given that the viscous damping of footbridge adopts Rayleigh damping, the decoupled single-degree-of-freedom equation corresponding to the nth mode of footbridge vibration is written as

$$\ddot{q}_n(t)+2\xi_n\omega_n\dot{q}_n(t)+\omega_n^2 q_n(t)=\frac{1}{M_n}\left\{\sum_{i=1}^{N}\sum_{k=1}^{K}\phi_n[(k-1)\Delta l+x_i]F_{ei}[t-(k-1)t_{si}-t_i]H(t,t_i)+\sum_{i'=1}^{N'}\sum_{k=1}^{K}\phi_n[(L-(k-1)\Delta l-x_i)]F_{ei'}[t-(k-1)t_{si'}-t_{i'}-\Delta T]H(t,t_{i'})\right\} \tag{13}$$

where ω_n, M_n and ξ_n are the nth modal circular frequency, modal mass, and modal damping ratio of footbridge. The time domain approach demonstrated above is costly even though a powerful computer is used to calculate the long-time vibration of footbridge. Additionally, as an indicator of the walking comfort of pedestrian, the rms acceleration is not clearly reflected in this time domain method. Therefore, in this paper, the time domain method only serves to examine the preciseness and efficacy of the more convenient random vibration model put forward in the next section.

4. Crowd-induced random vibration model

The randomness of the footbridge vibration, generated by crowd random walking, lies in the random stride rates and the random time intervals of neighboring pedestrians passing through the footbridge. From the study of time headway in the traffic flow, the gamma distribution [34] is adopted to describe the probability density function of the time intervals of neighboring pedestrians. By constructing the time sequence of walking pedestrians on the footbridge, the randomness of time interval is introduced to the crowd-induced random vibration model.

The vibration displacement is generally small when the footbridge vibrates vertically. Thus, it is difficult for the vertical vibration to induce the synchronism between the vibration phase of footbridge and the excitation phase of generalized force generated by crowd walking just like the mechanism of the lateral resonant vibration of slender footbridge. Additionally, the synchronism among the pedestrians is likely to occur when pedestrians queue to cross the footbridge in a congested state. In this particular synchronism, the walking speed of pedestrians will gradually tend to be identical, assuming that the stride lengths are generally the same, and thus the stride rates of pedestrians would be in complete agreement. As for the footbridge characterized with low vertical vibration frequency, the human walking comfort will be challenged seriously when the frequency of footbridge falls within the range of the frequency bandwidth of crowd-induced excitation. Therefore, in this model, stride rates of all the pedestrians are supposed to be the same and tuned to the natural frequencies of footbridge so as to excite the resonant or maximum vibration regarded as the control object of subsequent MTMD optimization.

Based on the assumptions above, the load excitation generated by crowd random walking equates with identical load time history in each standing point with the same time lag between two neighboring standpoints. Namely, the vibration of footbridge is equivalent to the vibration generated by completely coherent loading time history with identical time lag (travelling effect) in each standing point, as illustrated in Figs. 6 and 9. With a given value as their mean, a series of time intervals between neighboring walking pedestrians could be randomly generated by the traffic flow theory, and thus the loading time history generated by N pedestrians from the left end of footbridge in the first foot standpoint can be constructed by the single foot force model as

$$F_S(t) = F_{e1}(t) + \sum_{i=2}^{N} F_{ei}\left(t - \sum_{j=1}^{i-1} t_j\right), \quad t \geq 0 \tag{14}$$

where $F_{ei}(t)$ is the single foot force of the ith pedestrian. The loading time history in each foot standpoint can be transformed to loading power spectral density by FFT technique. Given that the stride rates of all pedestrians are the same, the loading power spectral density is merely dependent on the average time interval of walking pedestrians. Fig. 7 shows the load time history in the first standpoint when the average time interval is 2 s and the uniform stride rate is 2 Hz. Fig. 8 shows the loading power spectral densities corresponding to the different uniform stride rates 1.6, 2.0 and 2.4 Hz when the average time interval is 0.5 s. From Fig. 8, the loading power spectral density is focusedly distributed in the spectrum of threefold stride rates (1.6–7.2 Hz) while in other spectrum it is negligible. Thus, only the specific spectrum (1.6–7.2 Hz) of loading power spectral density is used to calculate the vibration response. Since the power spectral density is merely

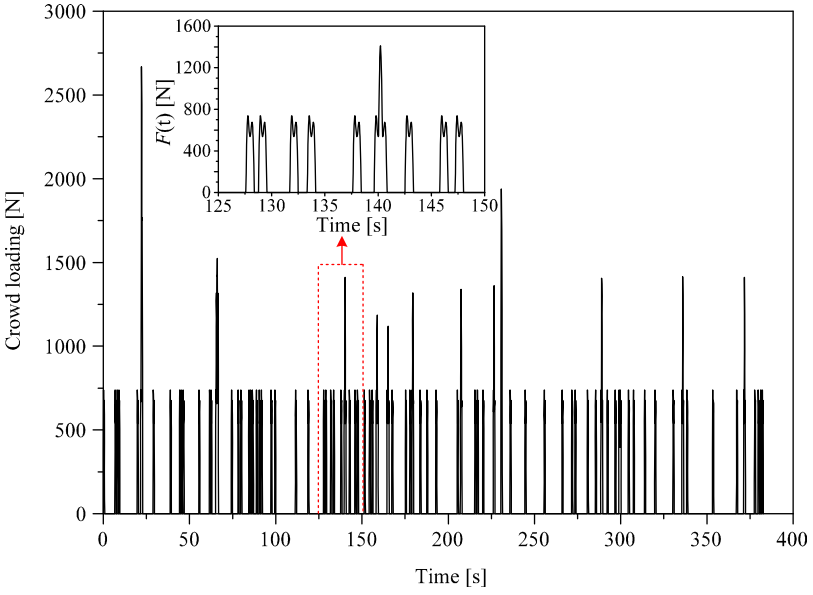

Fig. 7. Load time history in the first foot standpoint.

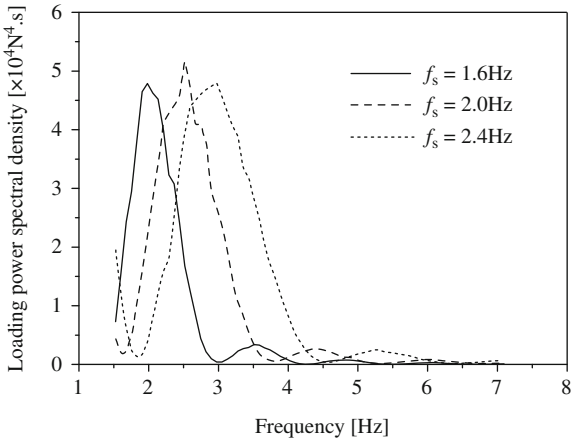

Fig. 8. Loading power spectral densities corresponding to different uniform stride rates.

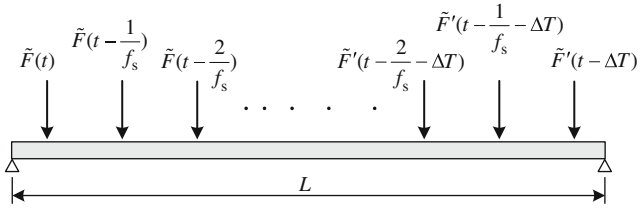

Fig. 9. The pseudo-excitation of two-way crowd walking.

dependent on uniform stride rate and average time interval, the footbridge vibration could be conveniently evaluated by studying these two parameters.

Illustrated in Fig. 6, the vertical motion of footbridge under random walking of crowd is

$$\frac{\partial^2}{\partial x^2}\left(EI\frac{\partial^2 u(x,t)}{\partial x^2}\right)+m\frac{\partial^2 u(x,t)}{\partial t^2}+c\frac{\partial u(x,t)}{\partial t}=\sum_{k=1}^{K}\delta(x-k\Delta l)F_S\left(t-\frac{(k-1)\Delta l}{\upsilon}\right)+\sum_{k=1}^{K}\delta(x-(L-k\Delta l))F_S\left(t-\frac{(k-1)\Delta l}{\upsilon'}-\Delta T\right),\quad \upsilon=f_s\Delta l,\ \upsilon'=f_s'\Delta l \tag{15}$$

where f_s and f_s' are the uniform stride rates of pedestrians from the left and the right, respectively; υ and υ' are the corresponding walking speeds. By the pseudo-excitation method [35], the pseudo-exciting force of $F_s(t)$ is written as

$$\tilde{F}_S(t)=\sqrt{S_{F_s}(\omega)}e^{i\omega t} \tag{16}$$

where $S_{F_n}(\omega)$ is the power spectral density of $F_s(t)$, illustrated in Fig. 8. By substituting Eq. (16) into Eq. (15), the vertical motion equation of footbridge expressed by pseudo-exciting force is written as

$$\frac{\partial^2}{\partial x^2}\left(EI\frac{\partial^2 \tilde{u}(x,t)}{\partial x^2}\right)+m\frac{\partial^2 \tilde{u}(x,t)}{\partial t^2}+c\frac{\partial \tilde{u}(x,t)}{\partial t}=\sum_{k=1}^{K}\delta(x-k\Delta l)\sqrt{S_{F_s}(\omega)}e^{i\omega(t-(k-1)/f_s)}+\sum_{k=1}^{K}\delta(x-(L-k\Delta l))\sqrt{S_{F_s}'(\omega)}e^{i\omega(t-(k-1)/f_s'-\Delta T)} \tag{17}$$

where $\tilde{u}(x,t)$ is the pseudo-displacement of footbridge. The pseudo-excitation of crowd walking is illustrated in Fig. 9, in which $\tilde{F}'(t)$ is the pseudo-exciting force induced by the right crowd walking. By decoupling Eq. (17), the nth modal equation of vertical motion is expressed as

$$\ddot{\tilde{q}}_n(t)+2\xi_n\omega_n\dot{\tilde{q}}_n(t)+\omega_n^2\tilde{q}_n(t)=\frac{1}{M_n}\sum_{k=1}^{K}(\phi_n(k\Delta L)\sqrt{S_{F_s}(\omega)}e^{i\omega(t-(k-1)/f_s)}+\phi_n(L-k\Delta L)\sqrt{S_{F_s}'(\omega)}e^{i\omega(t-(k-1)/f_s'-\Delta T)}) \tag{18}$$

where $\tilde{q}_n(t)$ is the pseudo nth modal coordinate of footbridge. From Eq. (18), $\tilde{q}_n(t)$ can be shown as

$$\tilde{q}_n(t)=\frac{\frac{1}{M_n}\sum_{k=1}^{K}(\phi_n(k\Delta L)\sqrt{S_{F_s}(\omega)}e^{i\omega(-(k-1)/f_s)}+\phi_n(L-k\Delta L)\sqrt{S'_{F_s}(\omega)}e^{i\omega(-((k-1)/f_s)-\Delta T)}\Big)}{\omega_n^2-\omega^2+2i\xi_n\omega_n\omega}e^{i\omega t} \tag{19}$$

After the superposition of all the modal responses, the pseudo-acceleration is written as

$$\ddot{\bar{u}}(x,t)=\sum_{n}^{\infty}\phi_n(x)\ddot{\bar{q}}_n(t) \tag{20}$$

Substituting Eqs. (19) into (20) results in the following pseudo-acceleration:

$$\ddot{\bar{u}}=-e^{i\omega t}\omega^2\left\{\sqrt{S_{F_s}(\omega)}\sum_{n}^{\infty}\frac{\phi_n(x)\sum_{k=1}^{K}\phi_n(k\Delta L)\{a_{nk}-ib_{nk}\}}{M_n[(\omega_n^2-\omega^2)^2+4\xi_n^2\omega^2\omega_n^2]}+\sqrt{S'_{F_s}(\omega)}\sum_{n}^{\infty}\frac{\phi_n(x)\sum_{k=1}^{K}\phi_n(L-k\Delta L)\{a'_{nk}-ib'_{nk}\}}{M_n[(\omega_n^2-\omega^2)^2+4\xi_n^2\omega^2\omega_n^2]}\right\} \tag{21}$$

where the intermediate variables are expressed as

$$\begin{aligned}
a_{nk}&=(\omega_n^2-\omega^2)\cos\left(\omega\left(\frac{k-1}{f_s}\right)\right)-2\zeta\omega_n\omega\sin\left(\omega\left(\frac{k-1}{f_s}\right)\right)\\
b_{nk}&=(\omega_n^2-\omega^2)\sin\left(\omega\left(\frac{k-1}{f_s}\right)\right)+2\zeta\omega_n\omega\cos\left(\omega\left(\frac{k-1}{f_s}\right)\right)\\
a'_{nk}&=(\omega_n^2-\omega^2)\cos\left(\omega\left(\frac{k-1}{f'_s}+\Delta T\right)\right)-2\zeta_n\omega_n\omega\sin\left(\omega\left(\frac{k-1}{f'_s}+\Delta T\right)\right)\\
b'_{nk}&=(\omega_n^2-\omega^2)\sin\left(\omega\left(\frac{k-1}{f'_s}+\Delta T\right)\right)+2\zeta_n\omega_n\omega\cos\left(\omega\left(\frac{k-1}{f'_s}+\Delta T\right)\right)
\end{aligned} \tag{22}$$

The acceleration power spectral density of footbridge at section x can be expressed as

$$S_{\ddot{u}}(x,w)=\ddot{\bar{u}}^{*}\ddot{\bar{u}} \tag{23}$$

where '*' symbolizes the conjugate complex operator. By substituting Eq. (21) into Eq. (23), the acceleration power spectral density becomes

$$\begin{aligned}
S_{\ddot{\bar{u}}}(x,\omega)=&\left\{\omega^2\sum_{n}^{\infty}\frac{\sqrt{S_{F_s}(\omega)}\phi_n(x)\sum_{k=1}^{K}\phi_n(k\Delta L)a_{nk}+\sqrt{S'_{Fs}(\omega)}\phi_n(x)\sum_{k=1}^{K}\phi_n(L-k\Delta L)a'_{nk}}{M_n[(\omega_n^2-\omega^2)^2+4\xi_n^2\omega^2\omega_n^2]}\right\}^2\\
&+\left\{\omega^2\sum_{n}^{\infty}\frac{\sqrt{S_{F_s}(\omega)}\phi_n(x)\sum_{k=1}^{K}\phi_n(k\Delta L)b_{nk}+\sqrt{S'_{Fs}(\omega)}\phi_n(x)\sum_{k=1}^{K}\phi_n(L-k\Delta L)b'_{nk}}{M_n[(\omega_n^2-\omega^2)^2+4\xi_n^2\omega^2\omega_n^2]}\right\}^2
\end{aligned} \tag{24}$$

Assuming that the acceleration time history at arbitrary position of footbridge is a stationary random process with the mean zero, the variance of acceleration is expressed as

$$\sigma^2_{\ddot{u}(x,t)}=E[\ddot{u}^2(x,t)]=\frac{1}{2\pi}\int_{-\infty}^{+\infty}S_{\ddot{\bar{u}}}(x,\omega)\,d\omega \tag{25}$$

And the rms acceleration is shown as

$$a_{\mathrm{rms}}=\sqrt{\frac{1}{T}\int_0^T a(t)^2\,dt} \tag{26}$$

Combining Eqs. (25) and (26) results in the rms acceleration:

$$a_{\mathrm{rms}}(x)=\sqrt{\frac{1}{2\pi}\int_{-\infty}^{+\infty}S_{\ddot{\bar{u}}}(x,\omega)\,d\omega} \tag{27}$$

Thus, the rms acceleration at arbitrary position of footbridge can be evaluated by the acceleration power spectral density expressed as Eq. (24).

This random vibration model can conveniently seize the resonant or maximum response of crowd–footbridge system, and what is more important, it can highly efficiently calculate the rms acceleration of footbridge under the worst crowd excitation. Based on this model, the MTMD design procedure considering the maximum rms acceleration of footbridge as the optimization objective is proposed.

5. Comparison between the time domain method and random vibration model

In order to verify the random vibration model mentioned above, the vibration analysis of one-span, two-equal-span and three-equal-span footbridges under crowd random walking are carried out and the maximum rms accelerations are compared between the time domain method and random vibration model. These three footbridges selected have the same main span, equal to 40 m, 2 Hz fundamental natural frequency, 0.01 damping ratio, 2400 kg/m line density, 9.96×10^9 Pa m^4 flexural stiffness and all boundary conditions are simply supported. An individual human weight is assumed to be

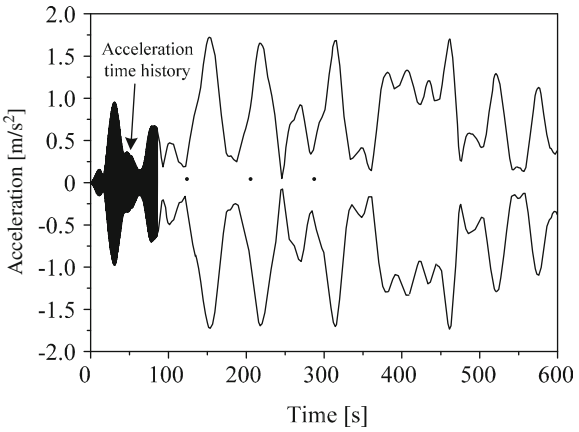

Fig. 10. The acceleration time history envelop of one-span footbridge in the midspan of mainspan.

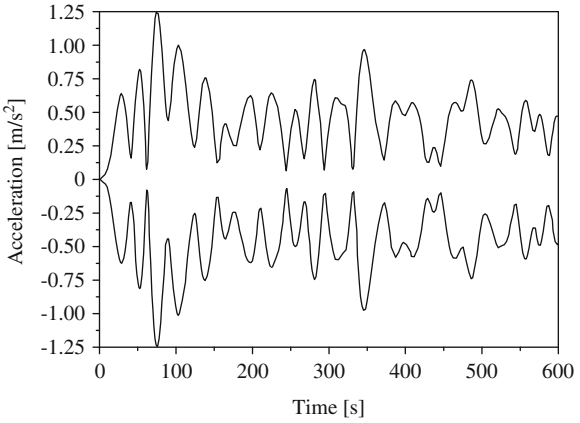

Fig. 11. The acceleration time history envelope of two-span footbridge in the midspan of mainspan.

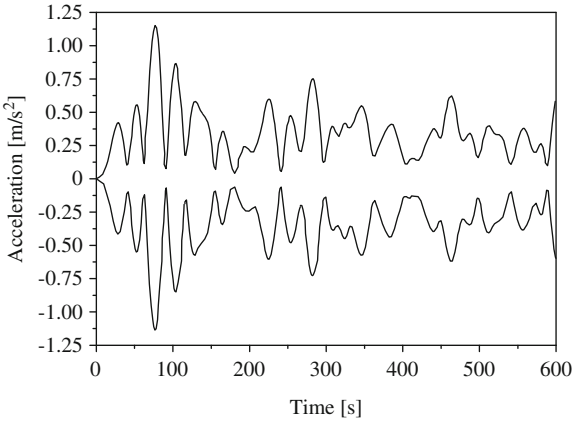

Fig. 12. The acceleration time history envelope of three-span footbridge in the midspan of mainspan.

700 N (0.7 kN), and the average time interval between neighboring pedestrians is adopted to 2 s, considering all the pedestrians move onto footbridge from the left end.

When the uniform stride rate of crowd coincides with the fundamental natural frequency of footbridge, the crowd–footbridge resonance will occur. Figs. 10–12 show the acceleration time history envelops of these three footbridges in the midspan of mainspan calculated by time domain method. The solution superposes the first three order modal responses, and the results show the response contribution of the first mode accounted for 97 percent of the superposed response,

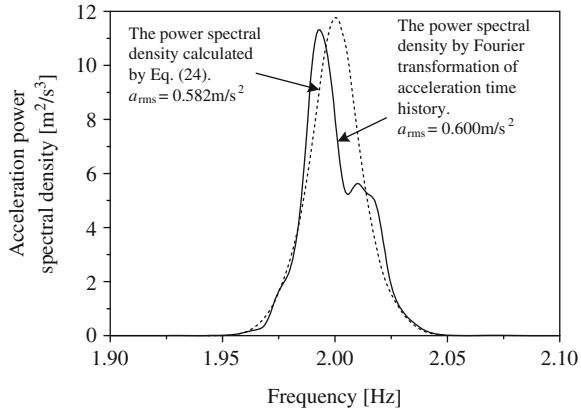

Fig. 13. Acceleration power spectral density comparison of one-span footbridge.

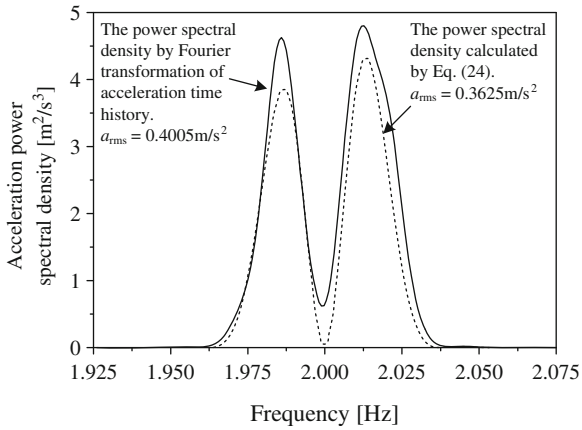

Fig. 14. Acceleration power spectral density comparison of two-equal-span footbridge.

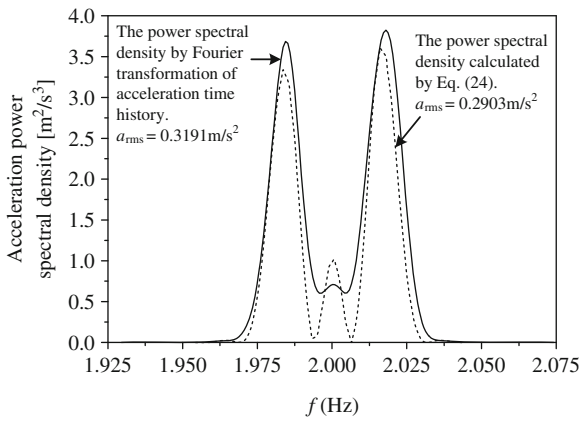

Fig. 15. Acceleration power spectral density comparison of three-equal-span footbridge.

which can be explained by the distantly spaced natural frequencies of footbridges and the closeness between the first modal frequency and stride rate of pedestrians. Correspondingly, Figs. 13–15 show the comparison between acceleration power spectral density transformed from the acceleration time histories presented in Figs. 10–12, and that calculated from Eq. (24). The acceleration power spectral density is focusedly distributed in the frequency range centering around footbridge fundamental frequency, implying that the first modal resonance of footbridge occurs. Due to some simplifications in the crowd-induced random vibration model, the acceleration power spectral density from the time

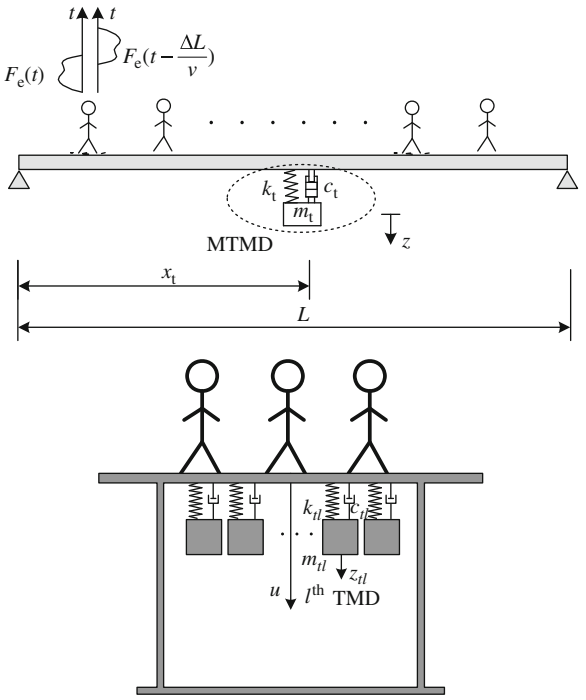

Fig. 16. Footbridge installed with multiple tuned mass damper system under crowd walking.

domain method is slightly greater than that from random vibration model, however, both the rms accelerations calculated by Eq. (27) are approximately equivalent. Therefore, the random vibration model is reasonable and applicable to evaluate the maximum rms acceleration of footbridge. In the other hand, comparing with the time domain method, the random vibration model is more advantageous in the computational efficiency and convenience.

6. Equations of motion for footbridge–MTMD system under crowd's random walking

The MTMD system with p parallelly placed tuned mass dampers is installed on the straight girder footbridge with length L at section $x=x_t$, as shown in Fig. 16. When a pedestrian flow is passing over the footbridge with the average time interval T from the left, the governing equations for the footbridge–MTMD system are given as follows:

1. The vertical motion equation at section x is similar to Eq. (9), with slight change of loading function due to the participation of MTMD. The changed loading function is

$$F(x,t)=\sum_{i=1}^{N}\sum_{k=1}^{K}\delta[x-(k-1)\Delta l-x_i]F_{ei}\left[t-(k-1)\frac{1}{f_{si}}-t_i\right]H(t,t_i)+\sum_{l=1}^{p}\delta(x-x_t)\{k_{tl}[z_{tl}-u(x_t,t)]+c_{tl}[\dot{z}_{tl}-\dot{u}(x_t,t)]\} \tag{28}$$

2. The vertical motion of the lth TMD is

$$m_{tl}\ddot{z}_{tl}(t)+c_{tl}[\dot{z}_{tl}(t)-\dot{u}(x_t,t)]+k_{tl}[z_{tl}(t)-u(x_t,t)]=0,\quad l=1,2,\ldots,p \tag{29}$$

In Eqs. (28) and (29), $u(x, t)$ and $z_{tl}(t)$ represent the vertical displacements of footbridge and the lth TMD. m_{tl}, c_{tl}, and k_{tl} represent the mass, damping coefficient, and stiffness of the lth TMD, respectively. In Eq. (28), the pedestrian is regarded as a moving force. If a moving mass model is used, the pedestrian load is written as

$$F'_{ei}=F_{ei}-\frac{G}{g}\ddot{u}(x_i(t),t) \tag{30}$$

where $x_i(t)$ is the position of the ith pedestrian on the footbridge. Due to the time variation of pedestrian's position on the footbridge, the load of pedestrian assumed as a moving mass is dependent on the displacement, velocity and acceleration of footbridge. This moving mass model reflects the interaction between footbridge and crowd, and can further estimate the time variance of footbridge modal frequency under crowd passing. Assuming the footbridge response consists of the modal responses of the first Q orders, the nth decoupled modal equation of vertical motion is expressed as

$$\ddot{q}_n(t)+2\xi_n\omega_n\dot{q}_n(t)+\omega_n^2q_n(t)=F_n(t)+F_{n,\mathrm{MTMD}}(t) \tag{31}$$

where the nth modal load function is

$$F_n(t)=\frac{1}{M_n}\sum_{i=1}^{N}\sum_{k}^{K}\phi_n[(k-1)\Delta l+x_i]F_{ei}[t-(k-1)t_{si}-t_i]H(t,t_i)$$

$$F_{n,\mathrm{MTMD}}(t)=\sum_{l=1}^{p}\mu_{tl,n}(\omega_{tl}^2 v_{tl}+2\xi_{tl}\omega_{tl}\dot{v}_{tl}) \tag{32}$$

In Eq. (32), $v_{tl}=z_{tl}-u(x_t,t)$, $\mu_{tl,n}=\phi_n(x_t)m_{tl}/M_n$; ω_{tl}, ξ_{tl}, v_{tl} and M_n represent the circular frequency, damping ratio, the stroke of the lth TMD and the nth modal mass of footbridge, respectively. Moreover, the coordinate in Eq. (29) can be rearranged into the stroke of the lth TMD as

$$\ddot{v}_{tl}+\sum_{n=1}^{Q}\phi_n(x_t)\ddot{q}_n(t)+2\xi_{tl}\omega_{tl}\dot{v}_{tl}+\omega_{tl}^2 v_{tl}=0 \tag{33}$$

Combining Eqs. (31) and (33), the coupled equations of motion in modal space are given in matrix form as

$$\begin{bmatrix}\mathbf{I}_{Q\times Q} & \mathbf{0}\\ \mathbf{M}_{ty} & \mathbf{I}_{P\times P}\end{bmatrix}\begin{Bmatrix}\ddot{\mathbf{q}}(t)\\ \ddot{\mathbf{v}}(t)\end{Bmatrix}+\begin{bmatrix}\mathbf{C}_{yy} & \mathbf{C}_{yt}\\ \mathbf{0} & \mathbf{C}_{tt}\end{bmatrix}\begin{Bmatrix}\dot{\mathbf{q}}(t)\\ \dot{\mathbf{v}}(t)\end{Bmatrix}+\begin{bmatrix}\mathbf{K}_{yy} & \mathbf{K}_{yt}\\ \mathbf{0} & \mathbf{K}_{tt}\end{bmatrix}\begin{Bmatrix}\mathbf{q}(t)\\ \mathbf{v}(t)\end{Bmatrix}=\begin{Bmatrix}\mathbf{F}(t)\\ \mathbf{0}\end{Bmatrix} \tag{34}$$

where

$$\mathbf{M}_{ty}^{\mathrm{T}}=\begin{bmatrix}\phi_1(x_t) & \phi_1(x_t) & \cdots & \phi_1(x_t)\\ \phi_2(x_t) & \phi_2(x_t) & \cdots & \phi_2(x_t)\\ \vdots & & \ddots & \vdots\\ \phi_Q(x_t) & \phi_Q(x_t) & \cdots & \phi_Q(x_t)\end{bmatrix},\quad \mathbf{C}_{yy}=\begin{bmatrix}2\xi_1\omega_1 & 0 & \cdots & 0\\ 0 & 2\xi_2\omega_2 & \cdots & 0\\ \vdots & & \ddots & \vdots\\ 0 & 0 & \cdots & 2\xi_Q\omega_Q\end{bmatrix}$$

$$\mathbf{C}_{yt}=\begin{bmatrix}-2\xi_{t1}\omega_{t1}\mu_{t1,1} & -2\xi_{t2}\omega_{t2}\mu_{t2,1} & \cdots & -2\xi_{tp}\omega_{tp}\mu_{tp,1}\\ -2\xi_{t1}\omega_{t1}\mu_{t1,2} & -2\xi_{t2}\omega_{t2}\mu_{t2,2} & \cdots & -2\xi_{tp}\omega_{tp}\mu_{tp,2}\\ \vdots & & \ddots & \vdots\\ -2\xi_{t1}\omega_{t1}\mu_{t1,Q} & -2\xi_{t2}\omega_{t2}\mu_{t2,Q} & \cdots & -2\xi_{tp}\omega_{tp}\mu_{tp,Q}\end{bmatrix}$$

$$\mathbf{C}_{tt}=\begin{bmatrix}2\xi_{t1}\omega_{t1} & 0 & \cdots & 0\\ 0 & 2\xi_{t2}\omega_{t2} & \cdots & 0\\ \vdots & & \ddots & \vdots\\ 0 & 0 & \cdots & 2\xi_{tp}\omega_{tp}\end{bmatrix},\quad \mathbf{K}_{yy}=\begin{bmatrix}\omega_1^2 & 0 & \cdots & 0\\ 0 & \omega_2^2 & \cdots & 0\\ \vdots & & \ddots & \vdots\\ 0 & 0 & \cdots & \omega_Q^2\end{bmatrix}$$

$$\mathbf{K}_{yt}=\begin{bmatrix}-\omega_{t1}^2\mu_{t1,1} & -\omega_{t2}^2\mu_{t2,1} & \cdots & -\omega_{tp}^2\mu_{tp,1}\\ -\omega_{t1}^2\mu_{t1,2} & -\omega_{t2}^2\mu_{t2,2} & \cdots & -\omega_{tp}^2\mu_{tp,2}\\ \vdots & & \ddots & \vdots\\ -\omega_{t1}^2\mu_{t1,Q} & -\omega_{t2}^2\mu_{t2,Q} & \cdots & -\omega_{tp}^2\mu_{tp,Q}\end{bmatrix}$$

$$\mathbf{K}_{tt}=\begin{bmatrix}\omega_{t1}^2 & 0 & \cdots & 0\\ 0 & \omega_{t2}^2 & \cdots & 0\\ \vdots & & \ddots & \vdots\\ 0 & 0 & \cdots & \omega_{tp}^2\end{bmatrix},\quad \mathbf{F}(\mathbf{t})=\begin{bmatrix}F_1(t)\\ F_2(t)\\ \vdots\\ F_Q(t)\end{bmatrix}$$

and $\mathbf{I}$ and $\mathbf{0}$ represent a unit matrix and a zero matrix. It should be brought to the notice that the global matrices in the equation above are asymmetric. It is a rare situation; the reason for that could possibly be the coupling between the vectors of $\mathbf{q}(t)$ and $\mathbf{v}(t)$. Eq. (34) is a general governing equation in modal space of the footbridge–MTMD system subjected to crowd walking excitation, and it is aimed to obtain the transfer function of footbridge and MTMD coupled response, which is essential to calculate the acceleration power spectral density and later the root-mean-square acceleration.

7. Dynamic characteristics of footbridge under crowd passing

When pedestrians are passing over the footbridge, the footbridge with the low natural frequency falling within the frequency bandwidth of crowd excitation will have a resonant effect and the footbridge natural frequency will change with time during crowd walking.

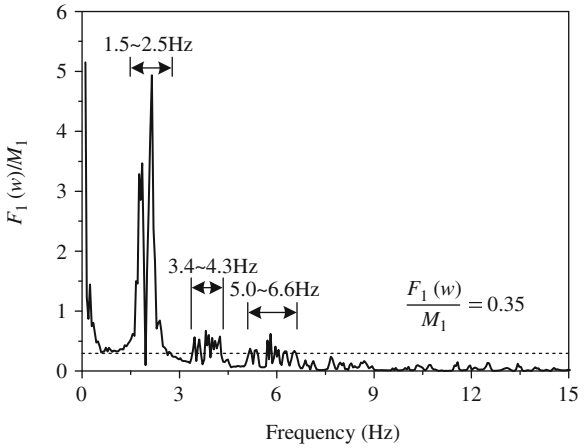

Fig. 17. Fourier transform of first modal crowd load with 2 s as the average time interval of the crowd flow.

7.1. Resonant frequency bandwidth of crowd walking excitation

In order to study the frequency bandwidth of crowd walking excitation, the spectral analysis of crowd load function is carried out and the main frequency bandwidth of crowd excitation is studied in this section. For instance, for the crowd flow with 2 s as its average time interval passing the one-span footbridge illustrated in Section 5 at the normally distributed stride rates with mean 2.0 Hz and standard deviation 0.173 Hz, the magnitude of the spectrum of the normalized first modal force, $|F_1(\omega)|/M_1$, is shown in Fig. 17. It is obviously seen that there exists peaks when the excitation frequency, f, is distributed in the frequency bandwidth of 1.5–2.5, 3.4–4.3, and 5.0–6.6 Hz, and the magnitudes of the spectrums of other modal forces have the similar characteristic. Accordingly, when the nth flexural modal frequency of footbridge is close to this frequency bandwidth, the crowd–footbridge resonance will occur. Therefore, it is necessary for the designer to verify whether the crowd–footbridge resonant response in the serviceability limit state meets the comfort requirement of pedestrian normal walking, and moreover whether the vibration control design is required, when the modal frequencies of footbridge fall within the resonant frequency bandwidth. Additionally, it is apparent to notice that the resonant effect could be avoided when the modal frequency of footbridge falls within the range of 2.5–3.4 Hz, though the natural frequency has a low magnitude. In other words, the vibration response of footbridge with its modal frequency in 2.5–3.4 Hz, is likely to be less intense than that of footbridge with its modal frequency in 3.4–4.3 or 5.0–6.6 Hz.

7.2. Time variation of footbridge modal frequency due to crowd random walking

The interaction between footbridge and crowd can be better described when adopting the more precise pedestrian model. For instance, applying a moving mass model for the pedestrian illustrated by Eq. (30), the equation of motion of the footbridge vertical displacement, Eq. (31), becomes

$$\mathbf{M}\ddot{\mathbf{q}}(\mathbf{t})+\mathbf{C}\dot{\mathbf{q}}(\mathbf{t})+\mathbf{K}\mathbf{q}(\mathbf{t})=\sum_{i=1}^{N}\sum_{k}^{K}\mathbf{\Phi}^{\mathrm{T}}[(k-1)\Delta l+x_i]H(t,t_i)\left\{F_{ei}[t-(k-1)t_{si}-t_i]-\frac{G}{g}\mathbf{\Phi}[(k-1)\Delta l+x_i]\ddot{q}(t)\right\} \tag{35}$$

or

$$[\mathbf{M}+\mathbf{M}'(t)]\ddot{\mathbf{q}}(t)+\mathbf{C}\dot{\mathbf{q}}(t)+\mathbf{K}\mathbf{q}(t)=\sum_{i=1}^{N}\sum_{k}^{K}\mathbf{\Phi}^{\mathrm{T}}[(k-1)\Delta l+x_i]H(t,t_i)F_{ei}[t-(k-1)t_{si}-t_i] \tag{36}$$

where $\mathbf{M}'(t)=\sum_{i=1}^{N}\sum_{k}^{K}\mathbf{\Phi}[(k-1)\Delta l+x_i]\mathbf{\Phi}^{T}[(k-1)\Delta l+x_i](G/g)H(t,t_i)$, $\mathbf{\Phi}^{\mathrm{T}}(x)=\{\phi_1(x),\ \phi_2(x),\ldots\}$. $\mathbf{M}$, $\mathbf{C}$ and $\mathbf{K}$ represent the modal mass matrix, modal damping matrix and modal stiffness matrix, respectively. When substituting Eq. (30) to Eq. (31), the terms corresponding to the displacement and velocity are ignored due to its trivial contribution compared to that of the acceleration term. It is evident that the mass matrix of the footbridge will be altered because of the participation of pedestrians. Furthermore, the mass matrix varies with time, which means that the modal frequency of footbridge will change with time during crowd passing. Fig. 18 shows the time variation of the first modal frequency of the one-span footbridge as presented in Section 5, subjected to a crowd flow with average time interval 0.5 s. Since the overall mass of footbridge increases as pedestrians pass over the footbridge, the system's natural frequencies are smaller than their original values. Though this interaction results in a change of the footbridge modal frequency, its variation is less than 1 percent of its original value. This indicates that the crowd walking even in a congested state does not lead to a significant change in the footbridge modal frequency to which the MTMD introduced in the next section is tuned.

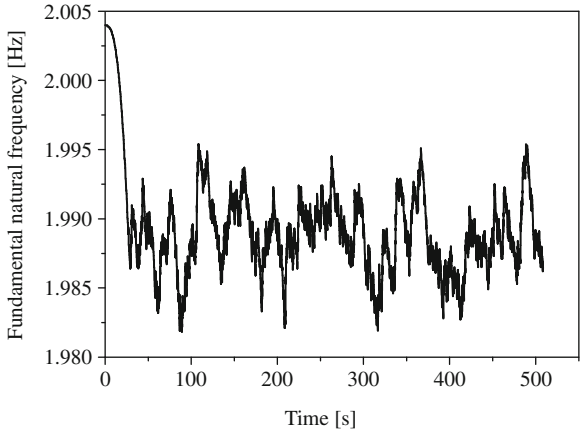

Fig. 18. Time variation of first modal frequency under crowd passing.

8. Optimization of multiple tuned mass dampers

Much research has been carried out to estimate the effectiveness of TMD in avoiding the excessive vibration of footbridge excited by pedestrian walking [20,23]. It is concluded that the optimal TMD is a useful control device in reducing excessive vibration when its frequency is well tuned to the resonant frequency of the footbridge. However, though the TMD vibration-reduced effectiveness is less useful outside the controlled frequency bandwidth, the footbridge vibration is in a low level. Additionally, it is also demonstrated that TMD's effectiveness was much sensitive to the frequency error to which TMD is tuned. The TMD's effectiveness degrades significantly if it does not right tune to the dominant frequency of footbridge. Thus, precise estimation of footbridge modal frequency is crucial to design the TMD control system. To overcome the deficiency of single TMD, the MTMD system consisting of multiple TMDs is developed to improve its reliability and robustness. Properly optimizing the MTMD parameters such as mass ratio, frequency ratio, and damping ratio, makes the MTMD system cover a wider frequency range than the single TMD system and thus be more robust to cover the controlled resonant frequency of footbridge, especially when the off-tuning effect exists and the footbridge is subjected to moderately wide-band crowd excitation.

When the modal frequencies of footbridge fall in the frequency bandwidth of crowd excitation, generally, these vibration modes should be controlled by MTMD system, respectively. In the vibration analysis, the MTMD system is put at the point with maximum structural response of the controlled mode shape [36], and the MTMD parameters are determined based on the minimization of maximum rms acceleration of footbridge when the total mass ratio of MTMD system and number of TMDs are determined. Since the crowd properties, such as the average time interval and distribution of stride rates are undefined, the optimized strategy is carried out assuming 0.5 s average time interval, which represents a congested walking state of footbridge [12]. According to the characteristic of crowd walking, the stride rates are normally distributed with mean 2.0 Hz, and standard deviation 0.173 Hz [11] when the footbridge has low crowd density. With the gradual increase of crowd density, the crowd stride rates produce a certain degree of synchronization among pedestrians [37], and moreover the crowd walking speeds tend to be the same when the crowd density increases to a high level. Due to the complexity of crowd stride rates and their synchronization, the MTMD optimized procedure takes account of two ultimate crowd stride rates distributions: (1) the crowd stride rates accord with normal distribution; (2) the uniform crowd stride rate obtains its value in [1.6, 2.4 Hz] so as to excite the worst resonant response of footbridge. These two scenarios can evaluate the most intense vibration of footbridge subjected to crowd excitation, and thus the optimized MTMD system only need to ensure the footbridge vibration below the vibration comfort requirement in these two scenarios.

8.1. Optimal multiple tuned mass damper parameters for footbridge under crowd walking with normally distributed stride rates

When considering the nth vertical mode of footbridge as a controlled mode of the MTMD system, taking the Fourier transform of Eqs. (34) yields the nth modal response of footbridge, $q_n(\omega)$, which is expressed as

$$q_n(\omega) = H_n^{\mathrm{MTMD}}(\omega) F_n(\omega) \tag{37}$$

The function $H_n^{\mathrm{MTMD}}(\omega)$ represents the transfer function of the nth modal displacement of footbridge corresponding to the nth modal crowd load $F_n(\omega)$. $H_n^{\mathrm{MTMD}}(\omega)$ is expressed as

$$H_n^{\mathrm{MTMD}}(\omega) = \frac{1}{(-\omega^2 + 2i\xi_n\omega_n\omega + \omega_n^2) - \sum_{l=1}^{p} \frac{\omega^2 \phi_n(x_t)\mu_{tl,n}(\omega_{tl}^2 + 2i\xi_{tl}\omega_{tl}\omega)}{-\omega^2 + 2i\xi_{tl}\omega_{tl}\omega + \omega_{tl}^2}} \tag{38}$$

The power spectral density of the nth flexural modal displacement and acceleration is written as

$$S_{q_n}(\omega) = H_n^{\mathrm{MTMD}}(\omega) S_{F_n}(\omega) (H_n^{\mathrm{MTMD}}(\omega))^* \tag{39}$$

$$S_{\ddot{q}_n}(\omega) = w^4 S_{q_n}(\omega) \tag{40}$$

where $S_{F_n}(\omega)$ is the power spectral function of nth modal force. And the maximum rms acceleration which corresponds to the rms acceleration in the midspan of footbridge is approximately expressed as

$$a_{\mathrm{rms}} = \sqrt{\frac{1}{2\pi}\int_{-\infty}^{\infty} S_{\ddot{q}_n}(\omega)\,\mathrm{d}\omega} \tag{41}$$

a_{rms}, as the general indicator of the walking comfort of pedestrian, is a function of $\phi_n(x_t)$, ξ_n (footbridge parameters) and ξ_{tl}, β_{tl}, $\mu_{tl,n}$ (MTMD parameters), where $\beta_{tl}=\omega_{tl}/\omega_n$ and $\mu_{tl,n}=m_{tl}/M_n$ is the modal frequency ratio and the modal mass ratio ($l=1,2,\ldots,p$). $\phi_n(x_t)$ can be determined by finding out the position of maximum response of the controlled mode shape. For simplifying the optimized procedure of MTMD parameters and convenient installation, the modal mass ratio of each TMD is assumed to be equal. Meanwhile, the total mass ratio, which equates with the sum of all modal mass ratios of TMDs, is generally chosen by taking both economy and the footbridge bearing capacity into consideration. For given values of $\phi_n(x_t)$ and ξ_n, the optimal MTMD parameters for the crowd stride rates normally distributed can be obtained by the following equations:

$$\begin{cases} \min \quad a_{\mathrm{rms}}(\xi_{tl},\beta_{tl}) = \sqrt{\frac{1}{2\pi}\int_{-\infty}^{\infty} S_{\ddot{q}_n}(\omega)\,\mathrm{d}\omega} \\ \text{s.t.} \quad 1 > \xi_{tl} > 0, \quad 2 > \beta_{tl} > 0 \quad (l = 1,2,\ldots,p) \\ \quad f_{si} \in N(2\,\mathrm{Hz}, 0.173\,\mathrm{Hz}) \quad (i = 1,2,\ldots,N) \end{cases} \tag{42}$$

8.2. Optimal multiple tuned mass damper parameters for footbridge under crowd passing with uniform stride rate

For the uniform crowd stride rate, the crowd flow only from the left is illustrated in Fig. 19. From the figure, the nth modal force is expressed as

$$F_n(t) = \frac{1}{M_n}\sum_{k=1}^{K} \phi_n(k\Delta l) F_S\left[t - \frac{(k-1)\Delta l}{v}\right], \quad v = f_s \Delta l \tag{43}$$

According to the pseudo-excitation method [35], the pseudo nth modal force is expressed as

$$\tilde{F}_n(t) = \frac{1}{M_n}\sum_{k=1}^{K} \phi_n(k\Delta l)\sqrt{S_{F_s}(\omega)}\,\mathrm{e}^{\mathrm{i}\omega(t-(k-1)\Delta l/v)} \tag{44}$$

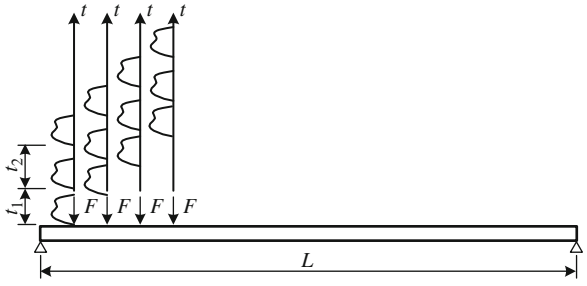

Fig. 19. Footbridge excited by foot standpoint loading generated by crowd walking.

Table 1
Definitions for GA optimization procedure.

N_{var}	Number of design variables
N_{sp}	Size of population
M_{cr}	Crossing rate
M_{mr}	Mutation rate
M_{mg}	Maximum number of generations

Thus, the power spectral density of the nth modal force is expressed as

$$S_{F_n}(\omega)=(\tilde{F}_n(t))^* * (\tilde{F}_n(t))=\frac{1}{M_n^2}\left[\sum_{k=1}^{K}\phi_n(k\Delta l)\sqrt{S_{F_s}(\omega)}e^{-i\omega(t-(k-1)\Delta l/v)}\right] * \left[\sum_{k=1}^{K}\phi_n(k\Delta l)\sqrt{S_{F_s}(\omega)}e^{i\omega(t-(k-1)\Delta l/v)}\right] \quad (45)$$

By combining Eqs. (39)–(41) and (45), the rms acceleration can be calculated. Accordingly, the optimal MTMD parameters for the uniform crowd rate can be determined by the following equations:

$$\begin{cases} \min \quad a_{\rm rms}(\xi_{tl},\beta_{tl})=\sqrt{\dfrac{1}{2\pi}\int_{-\infty}^{\infty}S_{\ddot{q}_n}(\omega)\,d\omega} \\ \text{s.t.} \quad 1>\xi_{tl}>0, \quad 2>\beta_{tl}>0 \quad (l=1,2,\ldots,p) \\ \quad f_{s1}=f_{s2}=\cdots=f_{sN}=f, \quad f\in[1.6,2.4]\,\text{Hz} \end{cases} \quad (46)$$

By comparing the optimization objectives in these two scenarios, the optimized MTMD parameters can be determined. In view of the inaccessibility of the derived function of optimization objective, the genetic algorithm is used to solve the above optimization problem presented by Eqs. (42) and (46). The essential parameter definitions for the employed GA optimization procedure in this study have been summarized in Table 1.

9. Numerical verification

The reduction of footbridge rms acceleration due to installation of the proposed optimal MTMD will be clearly illustrated in this section. Moreover, the off-tuning effect, resulting from footbridge frequency estimation error, on the MTMD control effectiveness will be extensively investigated.

Table 2
Parameters of GA optimization.

Optimal procedure	$N_{\rm var}$	$M_{\rm mr}$	$N_{\rm sp}$	$M_{\rm mg}$	$M_{\rm cr}$
1 TMD	2	0.05	20	50	0.95
3 TMDs	6	0.05	50	150	0.95
5 TMDs	10	0.05	100	300	0.95

Table 3
Optimal multiple tuned mass damper parameters for 2% total mass ratio and various numbers of tuned mass dampers (TMDs).

Number of TMDs, p	1	3	5
Optimal damping ratio, ξ_{t1}, $\xi_{t2},\ldots,\xi_{tp}$	0.0783	0.0478,0.1041,0.0517	0.036,0.0376,0.047,0.0478,0.0329
Optimal frequency ratio, β_{t1}, $\beta_{t2},\ldots,\beta_{tp}$	1.0027	0.9519,1.0372,1.0427	0.9331,0.966,1.0333,1.1335,1.0348
The maximum rms acceleration, $a_{\rm rms}$ (m/s^2)	0.2217	0.1874	0.1812

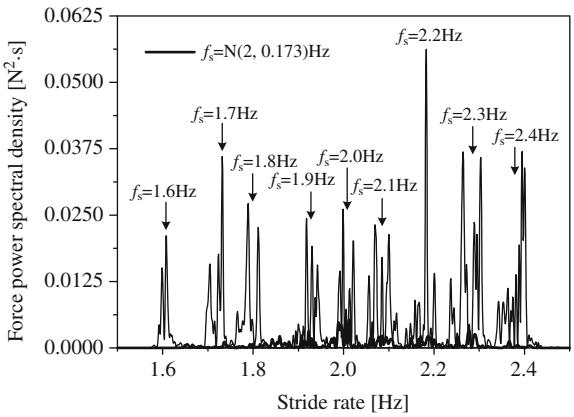

Fig. 20. Power spectral densities of modal generalized force for different distributions of crowd stride rate. (The thick continuous line are the crowd stride rates normally distributed with mean 2.0 Hz and standard deviation 0.173 Hz.)

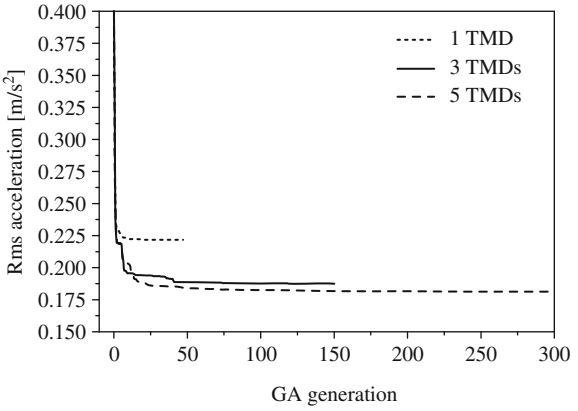

Fig. 21. GA optimization procedure for different number of TMDs.

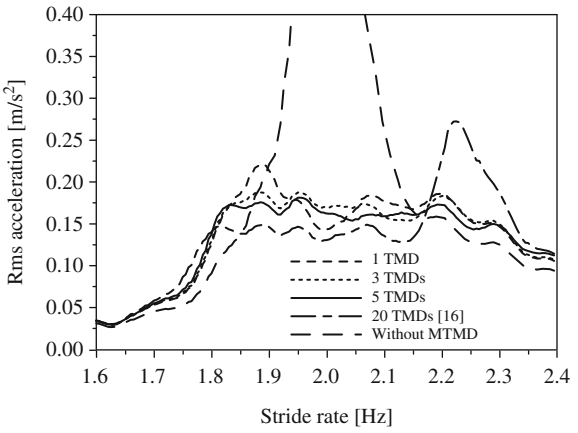

Fig. 22. Maximum rms acceleration of footbridge without and with single TMD, MTMD (p=3), MTMD (p=5), MTMD (p=20) [16].

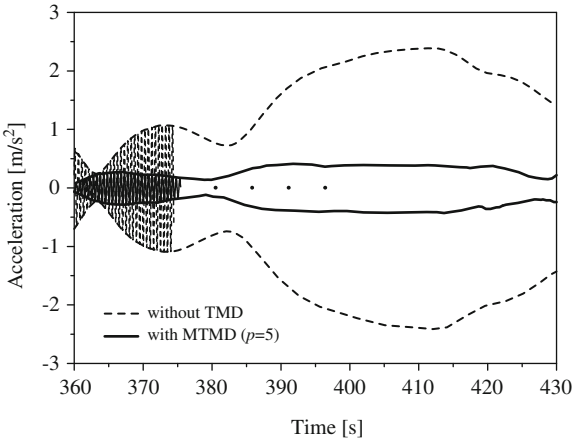

Fig. 23. Time history envelopes of acceleration at the midspan of footbridges without and with MTMD when the uniform stride rate is equal to the fundamental modal frequency of footbridge.

9.1. Multiple tuned mass damper control effectiveness for footbridge under crowd walking

It is obviously that when the modal frequency of footbridge falls within the resonant frequency bandwidth of crowd excitation, the corresponding resonant mode will be excited by crowd walking. Therefore, the MTMD is designed to control this resonant modal response which dominates the response of crowd–footbridge system, and is installed at the middle of the footbridge where the mode-shape value is maximum. The footbridge studied here is the one-span footbridge presented

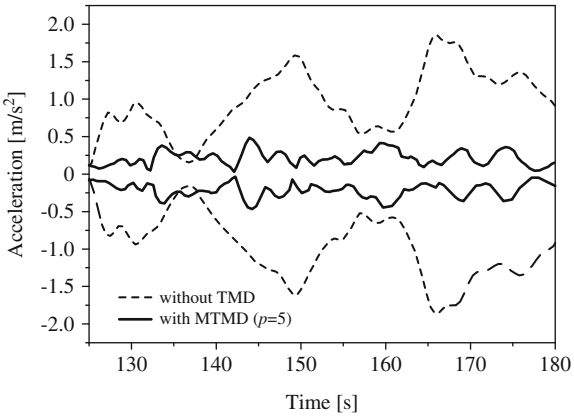

Fig. 24. Time history envelopes of acceleration at the midspan of footbridges without and with MTMD when stride rates are normally distributed.

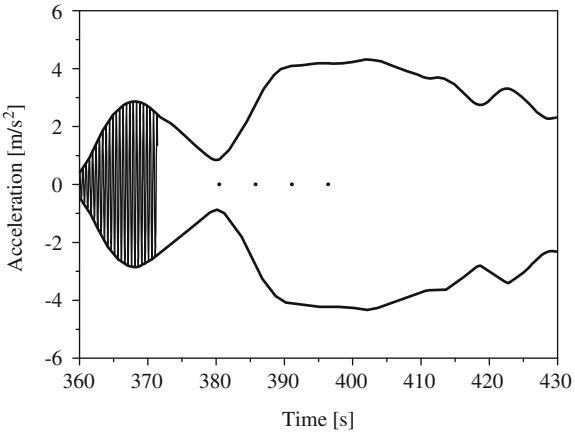

Fig. 25. Time history envelope of the most intense TMD acceleration when the uniform stride rate is equal to the fundamental modal frequency of footbridge.

in Section 5. MTMD system tunes to the first mode of footbridge and the total mass ratio of MTMD system is selected to be 2 percent. The detailed optimization procedures are illustrated in Fig. 21, and the corresponding parameters of GA optimization are listed in Table 2. The optimal parameters of MTMD with various number of TMDs resulting from the optimization strategy presented above are calculated and listed in Table 3. Corresponding to different stride rate distributions, the modal force power spectral densities of the controlled mode are illustrated in Fig. 20. It is seen that the power spectral densities are focusedly distributed in [1.6,2.4 Hz] which accords with the normal range of stride rate. According to the comparison of the optimized rms accelerations, respectively, resulting from Eqs. (42) and (46), the optimal design parameters of MTMD system are determined not by Eq. (42) (corresponding to normal distribution of stride rates) but by Eq. (46) (corresponding to the uniform stride rate). Thus, the most intense response of footbridge attached with MTMD system is determined by the crowd with the uniform stride rate on which the subsequent study of off-tuning effect is based. Fig. 22 presents the maximum rms acceleration curves of footbridge equipped with different vibration suppression systems among which the MTMD system designed by simply practical method [16] with frequency range 0.2, frequency spacing 0.01, total mass ratio 0.02 and damping ratio 0.01 is included when the crowd uniform stride rate ranges from 1.6 to 2.4 Hz. Since the simply practical method does not account for the damping of main structure and optimization procedure, its control effectiveness is slightly inferior to that of proposed MTMD systems in this paper. It is also shown that the maximum rms acceleration curve peak (0.875 m/s^2) for the footbridge without TMD is cut to a platform with wide frequency bandwidth for the footbridge with MTMD system. Compared with a single TMD, the MTMD with the same total mass ratio are more effective to reduce the footbridge rms acceleration. Due to the optimal MTMD system with 5 TMDs and 2 percent total mass ratio, the footbridge peak rms acceleration is approximately reduced to 20 percent original magnitude corresponding to the uncontrolled footbridge. The acceleration time history envelopes at the midspan of footbridge without and with MTMD are illustrated in Figs. 23 and 24. It is apparently found that the footbridge peak acceleration and acceleration level are both significantly reduced due to the proposed MTMD system. The most intense acceleration and stroke time history envelopes for all the TMDs (p=5) are also plotted in Figs. 25 and 26. It is seen that the TMD acceleration

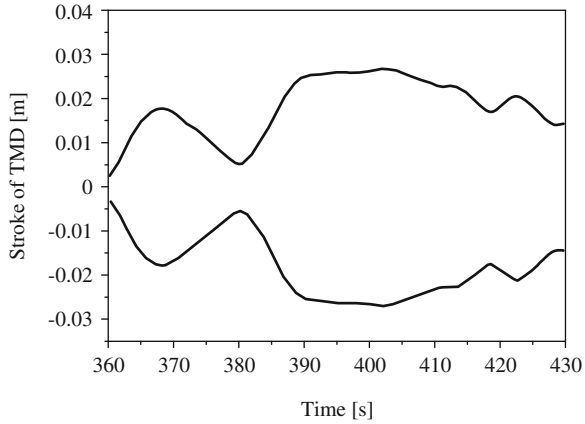

Fig. 26. Time history envelope of the most intense TMD stroke when the uniform stride rate is equal to the fundamental modal frequency of footbridge.

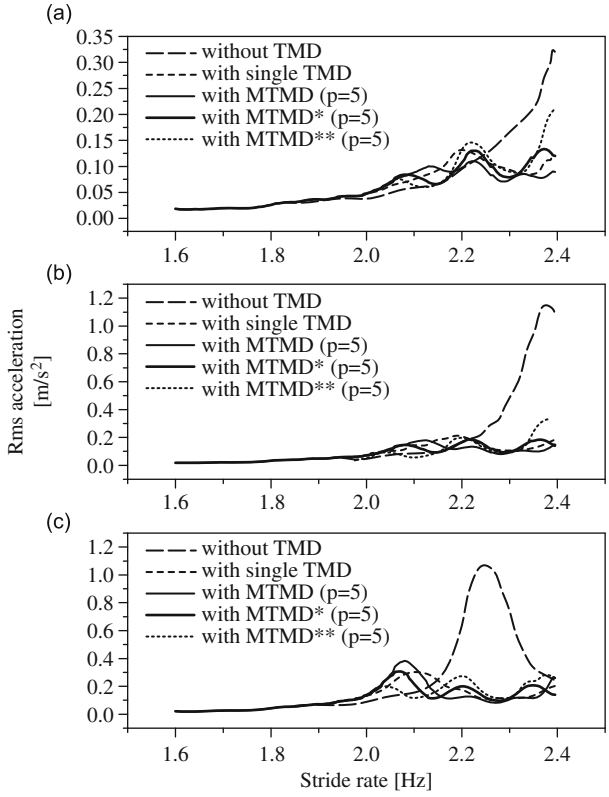

Fig. 27. Maximum rms accelerations without and with single TMD, MTMD and MTMD* when crowd uniform stride rate has its value from 1.6 Hz to 2.4 Hz. (a) Without off-tuning. (b) With −5% off-tuning. (c) With −10% off-tuning.

level is far beyond that of footbridge, and that the maximum stroke (0.028 m) is much smaller than the inner depth of footbridge girder. Therefore, there is enough space for installation and motion of the MTMD system.

9.2. Off-tuning effect

Though TMD is a high cost performance appliance and easy to install and maintain, however, the TMD control effectiveness will be degraded with time, resulting from the gradual disappearing of TMD viscous oil [38], changing of structure dynamic properties [20] and especially the structural natural frequency estimation error [18]. This is called the

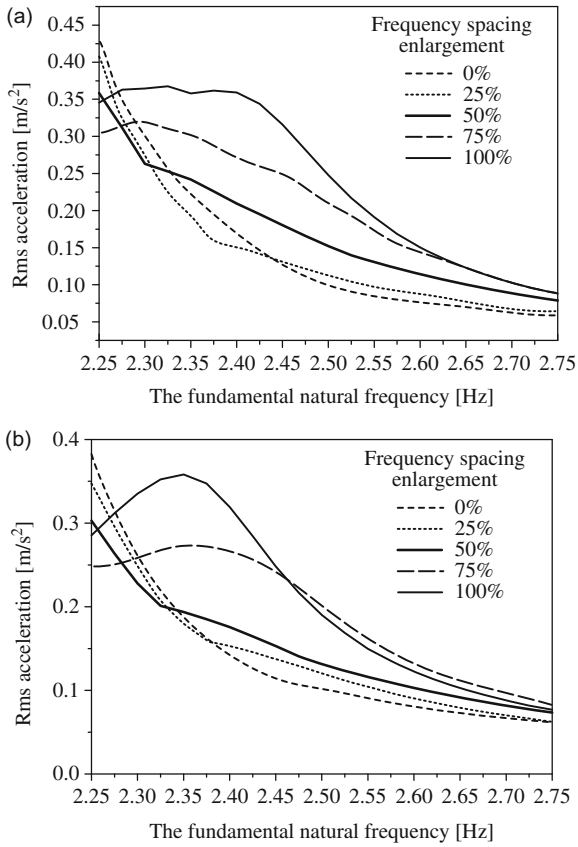

Fig. 28. Maximum rms accelerations for MTMD (p=3 and 5) with different frequency spacing enlargement considering frequency off-tuning. (a) MTMD* (p=3). (b) MTMD* (p=5).

off-tuning effect because TMD does not tune to the right frequency [18]. In order to guarantee the TMD control effectiveness in case of off-tuning effect, the MTMD system containing multiple tuning frequencies which create a wider frequency bandwidth is adopted to reduce the off-tuning effect. This section only investigates the MTMD off-tuning effect due to footbridge natural frequency change which is the most conducive factor to this effect.

To illustrate the reliability and robustness of MTMD system, the footbridge with the same layout presented in Section 9.1 except that the natural frequency is adopted to perform the numerical investigation. 2.5 Hz, which is the upper limit of the resonant frequency bandwidth, is chosen as the footbridge fundamental frequency to maximize the off-tuning effect. The maximum rms accelerations of footbridges without and with different MTMD systems are shown in Fig. 27 when off-tuning effect of varying degrees exists. From Fig. 27(a), it is obviously observed that both maximum rms accelerations of footbridges with single TMD or MTMD system are flattened significantly when no off-tuning effect exists. In order to increase the robustness of MTMD control effectiveness, another two MTMD systems (labeled as MTMD* and MTMD**) with the same center TMD frequency as the optimal MTMD system but respectively with 50 and 100 percent frequency spacing magnification between TMDs are proposed. The maximum rms acceleration curve corresponding to the MTMD* system is plotted in Fig. 27 as a thick solid line. For the case of no frequency off-tuning, the MTMD* and MTMD** systems are less effective to control the rms acceleration than the optimal MTMD system. However, when 5 or 10 percent frequency off-tuning exists, the control effectiveness of the optimal MTMD decreases significantly, whereas the MTMD* and MTMD** systems show little influence, as shown in Fig. 27(b) and (c). Fig. 28 presents the maximum rms accelerations of footbridges with MTMD (p=3 and 5) with varying frequency spacing enlargement when footbridge natural frequency off-tuning ranges from -10 to 10 percent . It is seen that MTMD* system has the better control effectiveness when natural frequency off-tuning exceeds 6 percent, although it will lose some control effectiveness in the case of no off-tuning or slight off-tuning. Therefore, in view of the significant frequency off-tuning, the proper frequency spacing enlargement of the optimal MTMD system can make the footbridge–MTMD system more reliable and robust.

10. Conclusion

When the footbridge natural frequencies fall within the frequency bandwidth of crowd excitation, illustrated in Fig. 17, generally the excessive vibration response due to crowd–footbridge resonance will exceed the normal walking comfort

requirement. To reduce the annoying vibration, the MTMD system is adopted. Based on the crowd–footbridge random vibration model, the general optimization procedure of optimal MTMD system is developed which takes account of the worst footbridge vibration state. For a congested crowd flow passing over a footbridge with different stride rate distributions, the optimal MTMD system has good control effectiveness when the frequency bandwidth of crowd excitation covers the modal frequency of footbridge. When the resonance does not happen, though the control effectiveness of MTMD system is not significant, the vibration response of footbridge is generally small enough to accord with the walking comfort requirement.

The study of the theoretical and numerical simulation presented in previous sections indicates that the following conclusions may be drawn:

(1) Based on Young and Ebrahimpour's researches on the characteristics of pedestrian-induced dynamic loads, the single foot force model presented by Fourier series is proposed. By comparing with series of measured walking forces, the recommended single foot force model has good accuracy and can be clearly adopted to analyze the footbridge vibration.
(2) According to the traffic flow theory, the crowd-induced random vibration model is developed. By comparing with the time domain method, the random vibration model has high effectiveness and can be conveniently used to evaluate the worst footbridge vibration response.
(3) When footbridge natural modal frequencies fall within the frequency bandwidth of crowd excitation (1.5–2.5, 3.4–4.3, and 5.0–6.6Hz), the crowd–footbridge resonance will occur even though the footbridge has a high fundamental frequency (more than 3 Hz).
(4) If the footbridge maximum rms acceleration is dominated by the crowd–footbridge resonance, the MTMD has good vibration control performance. As shown in Section 9.1, the peak rms acceleration of footbridge with MTMD system is approximately reduced to 20 percent the vibration response of footbridge without vibration control system.
(5) The estimation error of footbridge modal natural frequency has a notably disadvantageous effect on the TMD control effectiveness. The proposed MTMD system with proper frequency spacing enlargement is less influenced by the frequency off-tuning effect. Thus, it has the better reliability and robustness.

While offering an effective methodology for crowd-induced resonant vibration of footbridge, the proposed random vibration model needs to be further studied. For example, at present it is only applicable to compute the resonant vibration induced by crowd with uniform stride rate, and the movement correlation among different pedestrians with different crowd densities was not considered in the present application. Furthermore, when revealing the lateral resonant vibration mechanism of slender footbridge with low natural frequency of lateral vibration, this model ignores the correlation of footbridge vibration phase and crowd excitation phase. In its application, the loading power spectral density at foot standing point is required and, therefore, a Fourier transform code must be used. Nevertheless, the proposed model offers a highly efficient alternative to analyze crowd–footbridge vibration and the corresponding optimal MTMD system for vibration suppression.

Acknowledgments

The writers gratefully acknowledge the financial support provided by the National Science Fund of Beijing, China (8052013), Changjiang Scholars and Innovative Research Team in University (IRT00736).

References

[1] H. Bachmann, *Vibration Problems in Structures: Practical Guidelines*, Springer Verlag, 1995.
[2] J. Blanchard, B.L. Davies, J.W Smith, Design criteria and analysis for dynamic loading of footbridges, 1977.
[3] H. Bachmann, W. Ammann, *Vibrations in Structures—Induced by Man and Machines, Structural Engineering Documents*, Vol. 3e, International Association of Bridges and Structural Engineering (IABSE), Zurich, 1987.
[4] J.H. Rainer, G. Pernica, D.E. Allen, Dynamic loading and response of footbridges, *Canadian Journal of Civil Engineering* 15 (1) (1988) 66–71.
[5] S.C. Kerr, Human Induced Loadingon Staircases, PhD Thesis, Mechanical Engineering Department, University College London, UK, 1998.
[6] P. Young, Improved floor vibration prediction methodologies, ARUP Vibration Seminar, October 4, 2001.
[7] A. Ebrahimpour, A. Hamam, R.L. Sack, W.N. Patten, Measuring and modeling dynamic loads imposed by moving crowds, *Journal of Structural Engineering* 122 (12) (1996) 1468–1474.
[8] S. Zivanovi, A. Pavic, P. Reynolds, Probability-based prediction of multi-mode vibration response to walking excitation, *Engineering Structures* 29 (6) (2007) 942–954.
[9] S.V. Ohlsson, Floor Vibrations and Human Discomfort, PhD Thesis, Chalmers University of Technology, 1982.
[10] J. Brownjohn, A. Pavic, P. Omenzetter, A spectral density approach for modelling continuous vertical forces on pedestrian structures due to walking, *Canadian Journal of Civil Engineering* 31 (1) (2004) 65–77.
[11] Y. Matsumoto, T. Nishioka, H. Shiojiri, K. Matsuzaki, Dynamic design of footbridges, *IABSE Proceedings*, No. P-17/78, 1978, pp. 1–15.
[12] S.E. Mouring, B.R. Ellingwood, Guidelines to minimize floor vibrations from building occupants, *Journal of Structural Engineering* 120 (2) (1994) 507–526.
[13] F. Venuti, L. Bruno, N. Bellomo, Crowd dynamics on a moving platform: mathematical modelling and application to lively footbridges, *Mathematical and Computer Modelling* 45 (3–4) (2007) 252–269.

[14] Y. Fujino, B.M. Pacheco, S.I. Nakamura, P. Warnitchai, Synchronization of human walking observed during lateral vibration of a congested pedestrian bridge, *Earthquake Engineering & Structural Dynamics* 22 (9) (1993) 741–758.
[15] K. Xu, T. Igusa, Dynamic characteristics of multiple substructures with closely spaced frequencies, *Earthquake Engineering and Structural Dynamics* 21 (12) (1992) 1059–1070.
[16] H. Yamaguchi, N. Harnpornchai, Fundamental characteristics of multiple tuned mass dampers for suppressing harmonically forced oscillations, *Earthquake Engineering & Structural Dynamics* 22 (1) (1993) 51–62.
[17] M. Gu, S.R. Chen, C.C. Chang, Parametric study on multiple tuned mass dampers for buffeting control of Yangpu Bridge, *Journal of Wind Engineering & Industrial Aerodynamics* 89 (11–12) (2001) 987–1000.
[18] C.C. Lin, J.F. Wang, B.L. Chen, Train-induced vibration control of high-speed railway bridges equipped with multiple tuned mass dampers, *Journal of Bridge Engineering* 10 (4) (2005) 398–414.
[19] S.R. Chen, J. Wu, Performance enhancement of bridge infrastructure systems: long-span bridge, moving trucks and wind with tuned mass dampers, *Engineering Structures* 30 (11) (2008) 3316–3324.
[20] H. Bachmann, B. Weber, Tuned vibration absorbers for "Lively" structures, *Structural Engineering International* 5 (1) (1995) 31–36.
[21] N. Poovarodom, S. Kanchanosot, P. Warnitchai, Control of man-induced vibrations on a pedestrian bridge by nonlinear multiple tuned mass dampers, *The Eighth East Asia-Pacific Conference on Structural Engineering and Construction*, Paper no. 1344, Singapore, December 5–7, 2001.
[22] N. Poovarodom, C. Mekanannapha, S. Nawakijphaitoon, Vibration problem identification of steel pedestrian bridges and control measures, *Proceedings of the Third World Conference on Structural Control*, Como, Italy, April 7–12, 2002.
[23] N. Poovarodom, S. Kanchanosot, P. Warnitchai, Application of non-linear multiple tuned mass dampers to suppress man-induced vibrations of a pedestrian bridge, *Earthquake Engineering and Structural Dynamics* 32 (7) (2003) 1117–1131.
[24] International Organization for Standardization ISO 2631-2, Evaluation of Human Exposure to Whole-Body Vibration—Part 2: Continuous and Shock-Induced Vibration in Buildings (1–80 Hz), 1989.
[25] International Organization for Standardization ISO 10137, Bases for Design of Structures–Serviceability of Buildings Against Vibrations, 1992.
[26] T. Kobori, Y. Kajikawa, Ergonomic evaluation methods for bridge vibrations, *Transaction of JSCE* 6 (1974) 40–41.
[27] European Committee for Standardization, EN1990:2002. Eurocode, Basis of Structural Design, 2002.
[28] British Standards Association, BS 5400. Steel, Concrete and Composite Bridges, 1978.
[29] MTO, Ontario Highway Bridge Design Code (OHBDC), third ed., 1992.
[30] H. Bachmann, Vibration upgrading of gymnasia, dance halls and footbridges, *Structural Engineering International* 2 (2) (1992) 118–124.
[31] J. Blanchard, B.L. Davies, J.W. Smith, Design criteria and analysis for dynamic loading of footbridges, *Proceedings of the DOE and DOT TRRL Symposium on Dynamic Behaviour of Bridges*, Crowthorne, UK, May 19, 1977, pp. 90–106.
[32] Y. Matsumoto, S. Sato, T. Nishioka, H. Shiojiri, A study on design of pedestrian over-bridges, *Transactions of JSCE* 4 (1972) 50–51.
[33] R.W. Clough, J. Penzien, *Dynamics of Structures*, McGraw-Hill, New York, 1993.
[34] T. Luttinen, *Statistical Analysis of Vehicle Time Headways*, Teknillinen korkeakoulu, 1996.
[35] J.H. Lin, X.L. Guo, H. Zhi, W.P. Howson, F.W. Williams, Computer simulation of structural random loading identification, *Computers and Structures* 79 (4) (2001) 375–387.
[36] R.T. Jones, A.J. Pretlove, Vibration absorbers and bridges, *The Highway Engineer* 26 (2) (1979).
[37] S. Zivanovi, A. Pavic, P. Reynolds, Vibration serviceability of footbridges under human-induced excitation: a literature review, *Journal of Sound and Vibration* 279 (1–2) (2005) 1–74.
[38] R. Eyre, D.W. Cullington, Experience with vibration absorbers on footbridges, TRRL Research Report No. 18, Transport and Road Research Laboratory, Crowthrone, 1985.